Elsevier Editorial System(tm) for
Palaeogeography, Palaeoclimatology, Palaeoecology
Manuscript Draft

Manuscript Number:

Title: Depositional biofacies model for Aptian carbonate platforms of the western Maestrat Basin (Iberian Chain, Spain): a case history of post OAE1a Iberian platforms

Article Type: Research Paper

Keywords: Aptian; Carbonate platforms; Rudists; Paleoecology; Maestrat Basin; Spain

Corresponding Author: Dr. Eulàlia Gili,

Corresponding Author's Institution: Universitat Autonoma de barcelona

First Author: Eulàlia Gili

Order of Authors: Eulàlia Gili; Peter W Skelton; Telm Bover-Arnal; Ramon Salas; Antoni Obrador; Mükerrem Fenerci-Masse

Abstract: Two well exposed platform successions of late Early Aptian age developed in the central part of the Galve sub-basin (Maestrat Basin): the highstand platform (Camarillas-El Morrón), and the succeeding small lowstand platform (Las Mingachas), built out downslope in the former basin. Both platforms had a flat-topped non-rimmed depositional profile, showing similar platform-top to slope biofacies, which are described here in both qualitative and quantitative terms. The proximal platform top succession is characterized by a Toucasia-dominated rudist association. The margins of the two platforms consist of massive limestone characterized by a Polyconites-dominated association, in which clusters of Polyconites hadriani in life position are joined by both branching and domal corals, as well as the oyster-like Chondrodonta and nerineid gastropods. In Las Mingachas platform, where the massive rudist- and coral-rich platform limestones pass laterally into the slightly more marly and recessive clinoforms of the upper slope facies, Polyconites is especially abundant. Basinwards these slope deposits pass into basinal marls with orbitolinids and ammonoids. The distribution of the two distinct rudist associations recognized here is attributed to the different environmental tolerances of the rudists with respect to such factors as current regime and rate of sedimentation. The prevalence of polyconitids, in place of caprinids, in these late Early Aptian platform margin facies makes a striking contrast with older, earliest Aptian platforms.

Suggested Reviewers: Lucia Simone Dr
Professor, Dipartimento di Scienze della Terra, Università di Napoli ‘Federico II’
lusimone@unina.it
Professor Lucia Simone is an expert in carbonate stratigraphy and sedimentology. She has great experience in Cretaceous rudist platforms.

Robert W Scott Dr
Precision Stratigraphy Associates

rwscott@cimtel.net
Dr Robert W. Scott is an expert stratigrapher and palaeontologist. He has a considerable knownlwedge on Cretaceous rudist and coral platforms.

Pedro Angel Fernández-Mendiola Dr
Departamento de Estratigrafía y Paleontología, Universidad del País Vasco
kepa.fernandezmendiola@ehu.es
Dr Fernández-Mendiola, a stratigrapher and sedimentologist expert, works on Cretaceous rudist platforms in Iberia. The focus of his research have been on Aptian platforms.

Roberto Graciano Dr
Dipartimento di Scienze delle Terra, dell'Ambiente e delle Risorce, Università di Napoli Federici II
rgracian@unina.it
Dr R. Graciano is an expert in carbonate stratigraphy and sedimentology. His main research is on Aptian rudist platforms.

Tvrtko Korbar Dr
Croatian Geological Survey
Tvrtko.korbar@hgi.cgs.hr
Dr T. Korbar carries out research on rudist bivalve carbonate platforms. His works are mainly focused on stratigraphy, sedimentology and rudist palaeoecology.

Depositional biofacies model for Aptian carbonate platforms of the western Maestrat Basin (Iberian Chain, Spain): a case history of post OAE1a Iberian platforms

Eulàlia Gili[a], Peter W. Skelton[b], Telm Bover-Arnal[c], Ramon Salas[c], Antoni Obrador[a], Mükerrem Fenerci-Masse[d]

[a]Departament de Geologia, Facultat de Ciències, Universitat Autònoma de Barcelona, Edifici Cs, 08193, Bellaterra (Cerdanyola del Vallès), Spain. eulalia.gili@uab.cat, antoni.obrador@gmail.com

[b]Department of Environment, Earth and Ecosystems, The Open University, Milton Keynes MK7 6AA, UK. pwskelto@waitrose.com

[c]Departament de Geoquímica, Petrologia i Prospecció Geològica, Facultat de Geologia, Universitat de Barcelona, Martí i Franquès s/n, 08028, Barcelona, Spain. telm.boverarnal@ub.edu, ramonsalas@ub.edu

[d]CEREGE, Université de Aix-Marseille, Centre Saint Charles, 13331 Marseille Cedex 3, France. mugemasse@hotmail.com

Abstract

Two well exposed platform successions of late Early Aptian age developed in the central part of the Galve sub-basin (Maestrat Basin): the highstand platform (Camarillas-El Morrón), and the succeeding small lowstand platform (Las Mingachas), built out downslope in the former basin. Both platforms had a flat-topped non-rimmed depositional profile, showing similar platform-top to slope biofacies, which are described here in both qualitative and quantitative terms. The proximal platform top succession is characterized by a *Toucasia*-dominated

rudist association. The margins of the two platforms consist of massive limestone characterized by a *Polyconites*-dominated association, in which clusters of *Polyconites hadriani* in life position are joined by both branching and domal corals, as well as the oyster-like *Chondrodonta* and nerineid gastropods. In Las Mingachas platform, where the massive rudist- and coral-rich platform limestones pass laterally into the slightly more marly and recessive clinoforms of the upper slope facies, *Polyconites* is especially abundant. Basinwards these slope deposits pass into basinal marls with orbitolinids and ammonoids. The distribution of the two distinct rudist associations recognized here is attributed to the different environmental tolerances of the rudists with respect to such factors as current regime and rate of sedimentation. The prevalence of polyconitids, in place of caprinids, in these late Early Aptian platform margin facies makes a striking contrast with older, earliest Aptian platforms.

Keywords: Aptian, Carbonate platforms, Rudists, Paleoecology, Maestrat Basin, Spain

1. Introduction

The vast, low-latitude carbonate platforms of the globally encircling Cretaceous Atlantic-Tethys-Pacific oceanic belt have attracted considerable interest over the last few decades not only for their distinctive facies and biota (e.g., Simo et al., 1993; Gili et al., 1995) but also for what their episodic history of development and demise might tell us about the linkages between global oceanic, climatic and biotic changes (e.g., Skelton, 2003; Föllmi, 2012).

The Aptian Stage has attracted especial interest, as its rich and variegated record exemplifies the wide fluctuations of conditions experienced during the Cretaceous Period, of which it thus serves as a microcosm (Skelton and Gili, 2012). Within that context, Iberian platforms are of particular relevance, both in

occupying a palaeogeographical situation intermediate between those of the northern Tethyan margin and those of the central and southern Tethyan region, and in illustrating the biotic changes that took place throughout the Aptian Age, and especially during the crucial late Early Aptian interval following Oceanic Anoxic Event (OAE) 1a. Thick platform-bearing Aptian successions are spectacularly well-exposed in the Maestrat Basin and have been the subject of several detailed studies published during the last few decades (Canérot et al., 1982; Salas, 1987; Vennin and Aurell, 2001; Tomás et al., 2008; Bover-Arnal et al., 2009, 2010, 2011a, b, 2012, 2014, 2015, 2016; Embry et al., 2010; Martín-Martín et al., 2013; Peropadre et al., 2013). These works have been largely concerned with documenting the stratigraphy, sequence-stratigraphic architecture and facies of the successions and their relationships with regional and global events, and to a lesser extent with palaeoecological analysis of their biotic associations.

Complementing these previous studies, the present paper aims to address the last theme with respect to the platform sequences of late Early Aptian age that comprise the Villarroya de los Pinares Formation situated to the west of the village of Miravete de la Sierra, south of Aliaga in the province of Teruel (Fig. 1). After summarising the geological context within which these platform sequences were deposited and their consequent successions and facies architecture, we describe the compositions of the constituent biofacies in both quantitative and qualitative terms and then discuss the implications for understanding of the ambient environmental conditions in which they formed and the palaeoecology of the rudist bivalves that constitute their main macrobiotic elements.

2. Geological Setting of the study area

The study is focused on two successive Aptian (Early Cretaceous) carbonate platforms developed during two different stages of relative sea level change: (1) the highstand normal regressive (HNR) platform of *Camarillas-El Morrón*; and (2) the lowstand normal regressive (LNR) platform of *Las Mingachas* (Fig. 1). The platform deposits crop out in the environs of the villages of Camarillas and Miravete de la Sierra (Province of Teruel; E Spain) (Fig. 1A). A detailed geological context for these platform carbonates and the whole of the Aptian sedimentary succession where they are found is given in Bover-Arnal et al. (2009, 2010, 2011a, 2012, 2015, 2016), Moreno-Bedmar et al. (2009, 2010, 2012) and Garcia et al. (2014).

Fig. 1 here

The two carbonate platforms studied are located in the Galve sub-basin, on the western side of the Maestrat Basin in the eastern Iberian Chain (E Spain) (Fig. 1A). This basin developed as a result of Late Jurassic-Early Cretaceous rifting that affected the eastern Iberian Plate. During this time, a Mesozoic sedimentary succession up to a kilometre thick and ranging from continental to hemipelagic deposits accumulated in the basin. From the Paleogene to the Early Miocene, these Mesozoic deposits were inverted owing to the Alpine contraction, forming the Iberian Chain (Salas and Casas, 1993; Salas et al., 2001).

The platform carbonates studied herein correspond to the Villarroya de los Pinares Formation (Fig. 1B; Canérot et al., 1982). These rocks are characterized by floatstone and rudstone textures containing abundant scleractinian corals and rudist bivalves (Bover-Arnal et al., 2009, 2010). In the central Galve sub-basin, where the strata examined are found (Fig. 1A), the Villarroya de los Pinares Formation is of late Early Aptian age (intra *Dufrenoyia furcata* Zone) (Bover-Arnal et al., 2009, 2010, 2016; Moreno-Bedmar et al., 2010, 2012; Garcia et al., 2014). This formation changes both basinwards and downwards in the succession to the basinal marls of the Forcall Formation, which recorded the four Early Aptian ammonite zones (Fig. 1B; Moreno-Bedmar et al., 2010; Garcia et al., 2014; Bover-Arnal et al., 2016). On the other hand, the upper part of the Villarroya de los Pinares Formation passes laterally and upwards to latest Early-Late Aptian marls of the Benassal Formation (Fig. 1B; Bover-Arnal et al., 2012, 2016; Moreno-Bedmar et al., 2012; Garcia et al., 2014).

3. Platform architecture and context

Both of the uppermost Lower Aptian carbonate platform successions dominated by rudists and corals analysed here (Fig. 1C), had flat-topped, non-rimmed depositional profiles (Figs. 2 and 3), showing similar platform-top to slope biofacies stacked in a prograding pattern (Bover-Arnal et al., 2009).

The Camarillas-El Morrón platform succession (Sequence 'A') extends around 8 km NW-SE, from north of the village of Camarillas to El Morrón, in the vicinity of the village of Miravete de la Sierra, where the platform margin is situated, at Las Mingachas locality (Fig. 1A). It is of tabular form, and up to a maximum of nearly 35 m thick. Platform deposits pass southwestward to slope, then to basinal facies, exhibiting platform-to-slope clinoforms, which fade into basinal marls (Fig. 2).

Figs. 2 and 3 here

The small Las Mingachas carbonate platform (Sequence 'B'), located west of the village of Miravete de la Sierra (Fig. 1A), is for the most part 10 m thick and is traceable over an area of at least 0.16 km^2 (Fig 1C). The platform facies pass laterally to clinoforms representative of upper slope environments. Basinwards these slope deposits pass into basinal marls (Fig. 3).

In the Camarillas-El Morrón carbonate platform succession, marls and nodular marly limestones with abundant orbitolinids and ammonoids underlie the external parts of the platform and its margin. The proximal part of the platform (around Camarillas) overlies sandy limestones and calcarenites of shallow marine origin that display cross-bedding and plane-parallel stratification. The top of the preserved platform succession, visible in its proximal part, is capped by a composite stratigraphical surface, formed by a subaerial unconformity superposed by a hardground (maximum regressive surface, 'MRS') (Bover-Arnal et al., 2009; Fig. 4). This composite sequence boundary marks the

156 change in stacking pattern from progradation to retrogradation. In the most
157 internal parts of the platform, erosional incisions resulting from late Early Aptian
158 base-level fall are filled by cross-bedded and plane parallel stratified orange
159 calcarenites with abundant oysters, which represent peritidal transgressive
160 deposits of Sequence B (Fig. 4). Toward the platform margin, the upper part of
161 the platform is truncated by Cenozoic and/or Recent erosion.
162
163 Fig. 4 here
164
165 The composite stratigraphical surface that tops the Camarillas-El Morrón
166 carbonate platform splits into two surfaces toward the basin, the marine
167 correlative conformity below and the maximum regressive surface above (Fig.
168 5). These two surfaces bound the small Las Mingachas lowstand platform.
169 Above the correlative conformity ('CC'), this prograding carbonate platform
170 downlaps over a forced regressive wedge towards the basin and onlaps the
171 former slope of the Camarillas-El Morrón highstand platform landwards. The
172 lowstand platform is overlain by transgressive carbonates exhibiting
173 backstepping geometries (Figs. 1C and 5).
174
175 Fig. 5 here
176
177 **4. Methods**
178
179 In addition to conventional field investigation, logging and thin section analysis
180 of the studied sections by the first five authors, the sixth author (M.F.-M.) carried

out a quantitative fabric analysis of the rudist associations developed within them. The methodology employed for the latter analysis is explained in detail in Fenerci-Masse et al. (2004) and the variables measured are summarised in Table 1.

Table 1 here

Data analysis. Sample fabric relationships were investigated by principal component analysis (PCA) performed on the standardized variables. PCA is a multivariate technique for reducing matrices of data to a visually amenable form. It involves the condensation of a number of possibly correlated variables into a smaller number of uncorrelated variables called principal components. The first principal component accounts for as much of the variability in the data as possible (maximum variance direction), and each succeeding component accounts for as much of the remaining variability as possible. Projecting the data from their original dimensional space onto the dimensional subspace spanned by these principal components then reduces dimensionality with a minimum loss of information. A first plot, called the **correlation circle**, projects the initial variables on to the new factors space. It is useful in interpreting the meaning of the axes. A second plot shows the projection of row points (samples) on the new axes. The coordinates of samples on a significant number of axes (first two or three axes) were saved for subsequent hierarchical classifications.

The hierarchical classification of samples was made using Ward's method (Saporta, 1978) based on Euclidean distances between samples computed from their coordinates in each PCA (Roux, 1993, pp. 103–104; Lebart et al., 1995). These analyses were performed using the statistical software ADE-4 (Thioulouse et al., 1997).

Finally, in relation to the sequence stratigraphy, it should be noted that the terminology used in this paper follows the standardized nomenclature of genetic sedimentary units and sequence stratigraphic surfaces by Catuneanu et al. (2009), whereas Bover-Arnal et al. (2009, 2011a) previously applied the terminology found in the 'four-systems-tract' model of Hunt and Tucker (1992).

5. Results – description of biofacies

In many respects, the two studied carbonate platforms – the large prograding platform of Camarillas-El Morrón (Fig. 2) and the small prograding platform of Las Mingachas (Fig. 3) – resemble each other closely in terms of biofacies. But whereas the former platform is widely developed and shows a vertical evolution from thicker, aggrading, metre-scale, low energy platform top deposits to thinner, prograding, more marly beds, the latter platform lacks such a stratal development, owing to its lowstand genesis, and to its consequent limited thickness and lateral extent (few tens of metres, only). In this regard, the inner lowstand platform biofacies at Las Mingachas are somewhat similar to the platform margin and upper slope facies of the older but topographically higher highstand platform (Fig. 1C; Bover-Arnal et al., 2009, 2010, 2015). First, we

describe below the biofacies that characterize these platform settings and then interpret the environmental conditions in which they developed and the palaeoecological relationships between them, in the following section.

Two platform biofacies are readily distinguished in the field and are here named after the most abundantly represented rudist taxon in each case (Fig. 6). Assemblages in deposits corresponding to the more internal parts of the platform tops (at both Camarillas and Miravete de la Sierra) are dominated by the requieniid rudist *Toucasia carinata* (Fig. 6A). Deposits associated with the platform margins and upper slopes (seen only at Miravete de la Sierra) are, by contrast dominated by the polyconitid rudist *Polyconites hadriani* (Fig. 6B; see also Skelton et al., 2010). Accordingly we refer to them in the following discussion as the '*Toucasia*-', and the '*Polyconites* biofacies', respectively.

Fig. 6 here

Quantitative fabric analysis using PCA, followed by hierarchical classification, as explained in Section 4, was carried out on ten samples (field macro-photographs) in total, based on the data in Table 2. The *Toucasia* biofacies is represented by eight samples, six from the HNR internal platform at Camarillas ('Cam 1-6') and two from the internal part of the LNR platform at Miravete de la Sierra ('Mir 1-2'). A further two samples represent the *Polyconites* biofacies, both located at the margin of the LNR platform at Miravete de la Sierra ('Mir 3-4'). Results from this analysis are summarized in Figure 7, and their implications are incorporated in the descriptions of biofacies that follow.

Table 2 and Fig. 7 here

The first two axes of the PCA account for more than 87% of the observed variation in fabrics. Axis 1, accounting for 50% of the variation, displays, at its positive pole, the packing density, the skeletal contribution, coverage and the packing index, while Axis 2, accounting for 37% of the variation, expresses the increase of shell size (average, maximum and minimum) toward the positive pole (Fig. 7A, B). The clustering of these variables is shown in Fig. 7C.

The cluster analysis of samples (Fig. 7D) performed on the first three axes of the PCA reveals two associations of samples based on their physical characteristics. The first association, representing relatively dense assemblages of shells, groups two samples from the *Polyconites* biofacies at Miravete de la Sierra and two from the *Toucasia* biofacies at Camarillas. The discrete development of these genetically distinct dense associations in the two biofacies was based on their constituent rudist taxa, as described in the following sections. The second association comprises looser clusters of shells and includes two samples from Miravete de la Sierra and four from Camarillas, all from the *Toucasia* biofacies: these samples are all characterized by a low packing density and a low contribution of shelly material versus matrix**.**

5.1. Platform top biofacies

The internal platform top biofacies of the Camarillas-El Morrón carbonate platform are well exposed near Camarillas village (Figs. 1A and 8) and can be followed southwards for 8 km. The overwhelmingly dominant rudist taxon of this biofacies is the requieniid *Toucasia carinata* (Fig. 6A).

Above the basal cross-bedded sandy-limestones and calcarenites, the platform succession here continues with two successive units, which are separated by a sharp hardground surface (Fig. 8A, dashed line). Prior emersion of this surface, moreover, is suggested by the replacement of both geopetal cavity cements and the originally aragonitic inner shell in the rudists in unit 1 by red-stained fine-grained internal sediment (Fig. 8B).

Fig. 8 here

The first unit is a massive limestone bed, 6 m thick (Fig. 9A), with abundant displaced shells and fragments of *T. carinata* (Fig. 9B). According to the cluster analysis of Fig. 7D, both samples from this unit (Cam 1, 2), as well as the corresponding *Toucasia*-dominated biofacies in the lowstand platform at Miravete (Mir 1, 2) constitute relatively loosely clustered floatstone shell assemblages, with low values of packing index (max., 30.2%), skeletal contribution (max., 13.7%) and requieniid coverage (max., 29.4%) (Table 2). The *Toucasia* shells here are mostly isolated or are in small clusters and many are disarticulated or broken (Fig. 9B). The matrix of this biofacies varies from a marly fine bioclastic wackestone (Fig. 9C) to medium grained packstone (Fig. 9D). The bioclasts are predominantly plates and spines of echinoids and

304 fragments of rudists. Other frequent components are small benthic foraminifers
305 and, to a lesser extent, fragments of other molluscs, ostracodes and spicules of
306 sponges, and a very few orbitolinid foraminifers. All the bioclasts are angular,
307 though with well-developed micrite envelopes, implying extensive biological
308 boring but weak and infrequent current activity.
309
310 Fig. 9 here
311
312 Above the hardground capping the latter bed, the second unit comprises
313 repeated metre-scale cycles of marly limestone passing up to more resistant,
314 nodular bioclastic floatstone dominated by *Toucasia* (Figs. 8 and 10A). In these
315 *Toucasia* beds, the abundant spirally coiled shells of this clinger rudist (Gili et
316 al., 1995) – many still articulated (e.g., Fig. 6A) – show less evidence of
317 disturbance than those in the first unit, with parautochthonous to autochthonous
318 preservation (Fig. 10A). They were susceptible to storm disturbance, because
319 their basal surfaces were mainly only in frictional contact with the substrate,
320 although in a few instances the thickened basal anterior faces of their attached
321 (left) valves can also be seen encrusting hardground surfaces that cap some of
322 the cycles (Fig. 10B). Accompanying shelly macrofauna are rare elevator
323 rudists, including localized bouquets of small tubular monopleurids, *Mathesia*
324 sp. (Fig. 10C) and rare isolated specimens of *Polyconites hadriani* together with
325 a few small massive corals and rare branching corals (Fig. 10D). *In situ*
326 bouquets of the small tubular elevator *Mathesia* show relatively high values of
327 packing density, coverage and packing index (e.g., sample Cam 6; Table 2 and
328 Fig. 7).

Fig. 10 here

The combined emersion/hardground surface separating these two units (Fig. 8C, lower 'SU + MRS'), implying a succeeding slight transgressive increase in accommodation, could explain the enhanced marl accumulation and the growth of branching and massive corals, besides rudists, in unit 2.

5.2. Platform margin biofacies

The prograding margins of both platforms – characterized by the *Polyconites* association (Fig. 6B) – are formed of massive (~5m) limestones with both branching (phaceloid) and domal corals at their bases (Fig. 11A), followed upwards by clusters of *Polyconites hadriani* in life position (Fig. 11B), in turn covered by floatstones (Fig. 11C), the hard tops of which are locally encrusted by *Toucasia* (Fig. 11D).

Fig. 11 here

Quantitative analyses of a total vertical sectional area of 1,300 cm^2 of the polyconitid associations (e.g., Mir 4; Fig. 12) show a relatively high packing density, with a mean of 22 individuals per 100 cm^2 (2,200 individuals/m^2). Likewise, high values were recorded for packing index (averaging about 52%), skeletal contribution (around 24%) and polyconitid cover (around 50%) (Table 2).

Fig. 12 here

These closely packed clusters of *P*. *hadriani* are generally paucispecific, but may otherwise be joined locally by the elongated oyster-like (though unrelated) *Chondrodonta* (Fig. 11E) and nerineid gastropods. Also present are subsidiary *Toucasia*, which nevertheless becomes more abundant towards the upper part of the massive rudist and coral limestone, plus small tubular *Mathesia* sp., and rare caprinids, notably *Caprina parvula* (Fig. 11F) and *Offneria* sp., confirming the latest Bedoulian age of this unit (Bover-Arnal et al., 2010). The matrix is a poorly-sorted wackestone with plates and spines of echinoids, and rudist and coral fragments. Other components are small benthic foraminifers, a few dasycladaceans and localized crusts of microorganisms on coral fragments (Fig. 13).

Fig. 13 here

5.3. Slope biofacies

In both carbonate platforms, marginal facies change laterally into slope clinoforms (Figs. 2 and 3). Slope deposits consist of rudist and coral floatstones and rudstones with a matrix of fine-grained, poorly-washed grainstone to packstone with bioclasts of echinoids and thin-shelled bivalves (Fig. 14A, B). These limestone beds are interbedded with marls and marly limestones rich in

379 autochthonous coral colonies (see Bover-Arnal et al., 2012 for coral
380 descriptions). In the uppermost slope of the Camarillas-El Morrón platform,
381 autochthonous phaceloid corals (Fig. 14C) associated with *Polyconites hadriani*,
382 together with displaced *Toucasia*, are preserved within the floatstones.
383
384 Fig. 14 here
385
386 At Las Mingachas platform, where the massive rudist- and coral-rich platform
387 limestones pass laterally into the slightly more marly and recessive clinoforms
388 of uppermost slope facies, *Polyconites* is particularly abundant (Fig. 15A).
389 Locally, individuals are mutually attached preserved either in life position, in
390 dense clusters (Fig. 15B), together with a few platy corals (Fig. 15C), or as
391 overturned bouquets (Fig. 15D), accompanied by other skeletal debris.
392 Basinwards these slope deposits fade into basinal marls rich on orbitolinids and
393 ammonoids.
394
395 Fig. 15 here
396
397 **6. Interpretation of ambient conditions for biofacies and comments on the**
398 **ecology of the rudists**
399
400 Two distinct rudist associations have so far been recognized in the two
401 carbonate platforms investigated herein, based on taxonomic and biological
402 attributes (Section 5 Results – description of biofacies). The *Toucasia*
403 association, in the platform-top facies, is characterized by the dominance of the

requieniid *Toucasia carinata*, largely with low-packing density, low coverage of individuals and low contribution of shelly material versus matrix, although these variables are locally increased by interspersed bouquets of *Mathesia*. In the second, *Polyconites* association, which occupies the platform margin limestones, *Polyconites hadriani* is overwhelmingly dominant and is densely packed, covering a high percentage of surface area and contributing substantially to it relative to matrix.

The predominance of the clinger rudist *Toucasia carinata*, with a largely low-spiralling growth form (e.g., Fig. 10A) indicates a slow rate of sedimentation on the platform top. The mode of growth of clingers, maximising the basal area of direct contact with the substrate, required stable sedimentary, or hard surfaces and the relatively large proportion of displaced requieniid specimens moreover implies occasional (probably storm-related) current disturbance during deposition, especially in unit 1 of the HNR platform at Camarillas (Fig. 9B). The reduced disturbance of this kind in unit 2 at Camarillas (Fig. 10A) may reflect its greater distance from the open waters of the basin as a result of progradation of the HNR platform. Nevertheless, the fine-grained matrix textures of samples from the massive *Toucasia* bed of Camarillas unit 1 (Fig. 9C, D) and the subsidiary fauna of small elevator *Mathesia* and branching corals (Fig. 10C, D) found in the more marly, nodular beds of unit 2 testify that the background conditions were usually calm. We therefore interpret the platform-top biofacies, dominated by the requieniid rudists to have been deposited in relatively restricted shallow water – the unfavourable environmental conditions of which,

with respect to other biota', may explain its low biotic diversity – only sporadically disturbed by storms.

The greater diversity of fauna (i.e. diverse rudists, *Chondrodonta*, nerineid gastropods, corals) in the massive rudist- and coral-rich limestones at the platform margin of both sequences points to slightly deeper, more open waters, though the petrography of the matrix (a poorly sorted wackestone; Fig. 13) and the apparent lack of significant transport of bioclasts suggest moderately calm background conditions. However, occasional disturbance of rudist associations and *Chondrodonta* congregations by storm surges is evident from the floatstones (Fig. 11C).

The asymmetrically conical lower (right) valve and more or less flat upper valve of *Polyconites* allowed imbricate close-packing of individuals (Figs. 12 and 15A, B; Skelton et al., 2010), as in the living oyster *Crassostrea* (Fig. 16). This mode of growth would have assisted stabilization in areas of low net rate of sediment accumulation. Marginal bioclastic sediments were propitious for initial polyconitid colonization – as with all rudists, polyconitid spat needed a hard surface (e.g. a shell fragment) on which to settle (Hennhöfer et al., 2014) – and the hard surfaces of polyconitid shells and the nooks between the shells provided further places for new settlements. The apparently monospecific nature of the resulting *Polyconites hadriani* association may be due to the biochemical attraction of conspecific recruits by the previously established polyconitid individuals, as with living mussels (Bayne, 1964).

453 Fig. 16 here

454

455 An increase in the frequency of storm disturbance towards the top of the
456 massive limestone reflects a shallowing depositional trend in the marginal
457 carbonate sequence, which culminated in the establishment of the clinger
458 requieniid rudists on the platform top, well adapted to shallow-water conditions.

459

460 The gently sloping, marly sea floor of upper slope facies also favoured the
461 establishment of *Polyconites*. Here, the widespread and abundant polyconitids
462 are mostly congregated in small clusters or in bouquets of a few individuals
463 (Fig. 15D), presumably indicating sparse attachment sites. Sedimentation
464 appears to have been sporadic with *Polyconites* as well as the coral fauna
465 becoming established during lulls between influxes of sediment derived from the
466 shelf settings.

467

468 The prolific ‘oyster-like’ growth of *Polyconites hadriani* in the low wave-energy
469 platform margin and upper slope habitats of these carbonate platforms implies
470 an abundant supply of suspended food particles (phytoplankton,
471 microphytobenthos) (Skelton et al., 2010). Nutrient supply was probably
472 maintained by surficial water agitation, however resuspension of bacteria and
473 detrital organic particles may also have contributed considerably to sustain such
474 dense populations.

475

476 In summary, the biofacies recognized here, from *Polyconites*-dominated to
477 *Toucasia*-dominated, can be correlated with a sedimentary facies gradient

478 expressed both in lateral zonation and vertical succession. The different
479 environmental tolerances of the rudists relating to such factors as current
480 regime and rate of sedimentation determined their distribution in the carbonate
481 platform.
482 Interestingly, a somewhat contrasting biofacies pattern has recently been
483 documented for an isolated small platform situated just a few km to the south of
484 the present study area and correlated with Sequence A described herein
485 (Bover-Arnal et al., 2015). There, the inner platform was dominated by clusters
486 of slender elevator caprinids (*C. parvula*), while *Polyconites* and *Toucasia*
487 together predominated in the external zone. Reasons for this distinct pattern of
488 rudist colonization, at no great distance from the present study area, remain
489 unresolved at present, though the relatively purer carbonate matrix of the
490 caprinid facies in the isolated platform suggest that differences in the supply of
491 fine detrital sediment and/or associated nutrient flux could have been one
492 contributory factor. Whatever the reason for the difference, it illustrates the
493 diversity of ecological tolerances among rudist taxa that must always be
494 considered in studies of such platform associations (Skelton and Gili, 2012).
495

496 **7. Conclusions**

497

498 1. In the Maestrat Basin, the two carbonate platforms of late Early Aptian age,
499 the Camarillas-El Morrón highstand platform and the succeeding small Las
500 Mingachas lowstand platform, each show two distinct biofacies characterized by
501 two different rudist assemblages. In both cases, the requieniid rudist *Toucasia*
502 *carinata* dominates the carbonate deposits of the more internal parts of the

503 platform top, whereas the polyconitid rudist *Polyconites hadriani* dominates the
504 deposits of the platform margins and upper slopes.
505
506 2. The proximal to distal transition from requieniid-dominated to *Polyconites*-
507 dominated biofacies across the platforms reflects the influence of sedimentation
508 on the distribution of the different rudist palaeoecological morphotypes. The
509 relatively large clinger *Toucasia carinata* occupied the platform settings where
510 the net rate of sediment accumulation was low and sea-floor surfaces normally
511 stable, i.e. the inner platform top environments. In contrast, the elevator
512 *Polyconites hadriani* proliferated in more open waters with slightly higher rates
513 of sediment accumulation, in the moderately calm conditions of the platform
514 margins and upper slopes.
515
516 3. The prevalence of polyconitids in these late Early Aptian platform margin
517 facies, in particular, makes a striking contrast with older, earliest Aptian
518 platforms, and heralds the widespread proliferation of this group across the
519 Tethyan Realm through the Late Aptian and thereafter.
520
521
522 **Acknowledgements**
523
524 We acknowledge the financial support provided by Project I+D+i CGL2006-
525 02153 from the Ministerio de Educación y Ciencia, Spain and the Grup de
526 Recerca Reconegut per la Generalitat de Catalunya 2014 SGR 251 “Geologia
527 Sedimentària”.

528

529 **References**

530 Bayne, B.L., 1964. Primary and secondary settlement in *Mytilus edulis* L.
531 (Mollusca). Journal of Animal Ecology 33, 513–523.

532 Bover-Arnal, T., Salas, R., Moreno-Bedmar, J.A., Bitzer, K., 2009. Sequence
533 stratigraphy and architecture of a late Early-Middle Aptian carbonate platform
534 succession from the western Maestrat Basin (Iberian Chain, Spain).
535 Sedimentary Geology 219, 280–301.

536 Bover-Arnal, T., Salas, R., 2010. Outcrops with seismic-scale geometries: an
537 Aptian example from the western Maestrat Basin (E Iberia). 72nd EAGE
538 Conference & Exhibition incorporating SPE EUROPEC 2010, Barcelona, Spain,
539 14 - 17 June 2010. Abstracts J015.

540 Bover-Arnal, T., Moreno-Bedmar, J.A., Salas, R., Skelton, P.W., Bitzer, K., Gili,
541 E., 2010. Sedimentary evolution of an Aptian syn-rift carbonate system
542 (Maestrat Basin, E Spain): effects of accommodation and environmental
543 change. Geologica Acta 8, 249–280.

544 Bover-Arnal, T., Salas, R., Skelton, P.W., Gili, E., Moreno-Bedmar, J.A., 2011a.
545 The Aptian carbonate platforms of the western Maestrat Basin: a textbook
546 example of four systems tract-based sequence stratigraphy, in: Arenas, C.,
547 Pomar, L., Colombo, F. (Eds), Pre-Meeting Field trips Guidebook, 28th IAS
548 Meeting, Zaragoza Sociedad Geológica de España, Geo-Guías 7, pp. 27–64.

549 Bover-Arnal, T., Salas, R., Martín-Closas, C., Schlagintweit, F., Moreno-Bedmar,
550 J.A., 2011b. Expression of an oceanic anoxic event in a neritic setting: Lower

Aptian coral rubble deposits from the western Maestrat Basin (Iberian Chain, Spain). Palaios 26, 18–32.

Bover-Arnal, T., Löser, H., Moreno-Bedmar, J.A., Salas, R., Strasser, A., 2012. Corals on the slope (Aptian, Maestrat Basin, Spain). Cretaceous Research 37, 43–64.

Bover-Arnal, T., Salas, R., Guimerà, J., Moreno-Bedmar, J.A., 2014. Deep incision on an Aptian carbonate succession indicates major sea-level fall in the Cretaceous. Sedimentology 61, 1558–1593.

Bover-Arnal, T., Pascual-Cebrian, E., Skelton, P.W., Gili, E., Salas, R., 2015. Patterns in the distribution of Aptian rudists and corals within a sequence-stratigraphic framework (Maestrat Basin, E Spain). Sedimentary Geology 321, 86-104.

Bover-Arnal, T., Moreno-Bedmar, J.A., Frijia, G., Pascual-Cebrian, E., Salas, R., 2016. Chronostratigraphy of the Barremian-Early Albian of the Maestrat Basin (E Iberian Peninsula): integrating strontium-isotope stratigraphy and ammonoid biostratigraphy. Newsletters on Stratigraphy.

Canérot, J., Crespo, A., Navarro, D., 1979. Montalbán, hoja nº 518. Mapa Geológico de España 1:50.000. 2ª Serie. 1ª Edición. Servicio de Publicaciones, Ministerio de Industria y Energía, Madrid, 31 pp.

Canérot, J., Cugny, P., Pardo, G., Salas, R., Villena, J., 1982. Ibérica Central-Maestrazgo, in: García, A. (Ed.), El Cretácico de España. Universidad Complutense de Madrid, pp. 273–344.

574 Catuneanu, O., Abreu, V., Bhattacharya, J.P., Blum, M.D., Dalrymple, R.W.,
575 Eriksson, P.G., Fielding, C.R., Fisher, W.L., Galloway, W.E., Gibling, M.R.,
576 Giles, K.A., Holbrook, J.M., Jordan, R., Kendall, C.G.St.C., Macurda, B.,
577 Martinsen, O.J., Miall, A.D., Neal, J.E., Nummedal, D., Pomar, L., Posamentier,
578 H.W., Pratt, B.R., Sarg, J.F., Shanley, K.W., Steel, R.J., Strasser, A., Tucker,
579 M.E., Winker, C., 2009. Towards the standardization of sequence stratigraphy.
580 Earth-Science Reviews 92, 1–33.
581 Fenerci-Masse, M., Masse, J.-P., Chazottes, V., 2004. Quantitative analysis of
582 rudist assemblages: a key for palaeocommunity reconstructions. The Late
583 Barremian record from SE France. Palaeogeography, Palaeoclimatology,
584 Palaeoecology 206, 133-147.

585 Flügel, E., 1982. Microfacies analysis of limestones. Springer Verlag, Berlin.

586 Garcia, R., Moreno-Bedmar, J.A., Bover-Arnal, T., Company, M., Salas, R.,
587 Latil, J.L., Martín-Martín, J.D., Gomez-Rivas, E., Bulot, L.G., Delanoy, G.,
588 Martínez, R., Grauges, A., 2014. Lower Cretaceous (Hauterivian-Albian)
589 ammonite biostratigraphy in the Maestrat Basin (E Spain). Journal of Iberian
590 Geology 40, 99-112.

591 Gautier, F., 1980. Villarluengo, hoja nº 543. Mapa Geológico de España
592 1:50.000. 2ª Serie. 1ª Edición. Servicio de Publicaciones, Ministerio de Industria
593 y Energía, Madrid, 45 pp.

594 Gili, E., Masse, J.-P., Skelton, P.W**.,** 1995. Rudists as gregarious sediment-
595 dwellers, not reef-builders, on Cretaceous carbonate platforms.
596 Palaeogeography, Palaeoclimatology, Palaeoecology 118, 245–267.

Hennhöfer, D. K., Pascual–Cebrian, E., Korbar,T., Stinnesbeck, W., Götz, S., 2014. Radiolitid rudist colonisation strategies and biostrome development in moderate–energy inner–platform environments (Campanian, Brač Island, Croatia). Palaeogeography, Palaeoclimatology, Palaeoecology 403, 80–87.

Hunt, D., Tucker, M.E., 1992. Stranded parasequences and the forced regressive wedge systems tract: deposition during base-level fall. Sedimentary Geology 81, 1-9.

Lebart, L., Morineau, A., Piron, M., 1995. Statistique exploratoire multidimensionnelle. Dunod, Paris.

Martín-Martín, J.D., Gomez-Rivas, E., Bover-Arnal, T., Travé, A., Salas, R., Moreno-Bedmar, J.A., Tomás, S., Corbella, M., Teixell, A., Vergés, J., Stafford, S.L., 2013. The Upper Aptian to Lower Albian synrift carbonate succession of the southern Maestrat Basin (Spain): Facies architecture and fault-controlled stratabound dolostones. Cretaceous Research 41, 217–236.

Moreno-Bedmar, J.A., Company, M., Bover-Arnal, T., Salas, R., Delanoy, G., Martínez, R., Grauges, A., 2009. Biostratigraphic characterization by means of ammonoids of the lower Aptian Oceanic Anoxic Event (OAE1a) in the eastern Iberian Chain (Maestrat Basin, eastern Spain). Cretaceous Research 30, 864-872.

Moreno-Bedmar, J.A., Company, M., Bover-Arnal, T., Salas, R., Maurrasse, F.J., Delanoy, G., Grauges, A., Martínez, R., 2010. Lower Aptian ammonite biostratigraphy in the Maestrat Basin (Eastern Iberian Chain, Eastern Spain). A

621 Tethyan transgressive record enhanced by synrift subsidence. Geologica Acta
622 8, 281–299.

623 Moreno-Bedmar, J.A., Bover-Arnal, T., Barragán, R., Salas, R., 2012.
624 Uppermost Lower Aptian transgressive records in Mexico and Spain:
625 chronostratigraphic implications for the Tethyan sequences. Terra Nova 24,
626 333–338.

627 Pérés, J.M., 1961. Océanographie biologique et biologie marine. T. 1: La vie
628 benthique. Presses Univ. France, Paris.

629 Roux, M., 1993. Classification des données d'enquêtes, in : Grangé, D., Lebart,
630 L. (Eds.), Traitements statistiques des enquêtes. Dunod, Paris.

631 Salas, R., 1987. El Malm i el Cretaci inferior entre el Massís de Garraf i la Serra
632 d'Espadà. Anàlisi de Conca. PhD thesis, Universitat de Barcelona, 345 p.
633 Salas, R., Casas, A., 1993. Mesozoic extensional tectonics, stratigraphy, and
634 crustal evolution during the Alpine cycle of the eastern Iberian basin.
635 Tectonophysics 228, 33–55.

636 Salas, R., Guimerà, J., Mas, R., Martín-Closas, C., Meléndez, A., Alonso, A.,
637 2001. Evolution of the Mesozoic Central Iberian Rift System and its Cainozoic
638 inversion (Iberian Chain), in: Ziegler, P.A., Cavazza, W., Roberston, A.H.F.,
639 Crasquin-Soleau, S. (Eds.), Peri-Tethys Memoir 6: Peri-Tethyan Rift/Wrench
640 Basins and Passive Margins. Mémoires du Muséum National d'Histoire
641 Naturelle, Paris, 186, pp. 145–186.

642 Saporta, G., 1978. Théories et methods de la statistique. Technip, Paris.

643 Simo, J.A.T., Scott, R.W., Masse, J.-P., 1993. Cretaceous carbonate platforms:
644 an overview, in: Simo, J.A.T., Scott, R.W., Masse, J.-P. (Eds.), Cretaceous
645 carbonate platforms. AAPG Mem., 56, pp. 1-14.

646 Skelton, P.W. (Ed.), 2003. The Cretaceous World. Cambridge University Press
647 and The Open University.

648 Skelton, P.W., Gili, E Bover-Arnal, T., Salas, R., Moreno-Bedmar, J.A., 2010. A
649 new species of *Polyconites* from the Lower Aptian of Iberia and the early
650 evolution of polyconitid rudists. Turkish Journal of Earth Sciences 19, 557-572.

651 Skelton, P.W., Gili, E., 2012. Rudists and carbonate platforms in the Aptian: a
652 case study on biotic interactions with ocean chemistry and climate.
653 Sedimentology 59, 81–117.

654 Thioulouse, J., Chessel, D., Dolédec, S., Olivier, J.M., 1997. ADE-4: a
655 multivariate analysis and graphical display software. Stat. Comput. 7, 75-83.

656 Tomás, S., Löser, H., Salas, R., 2008. Low-light and nutrient-rich coral
657 assemblages in an Upper Aptian carbonate platform of the southern Maestrat
658 Basin (Iberian Chain, eastern Spain). Cretaceous Research 29, 509–534.

659 Vennin, E., Aurell, M., 2001. Stratigraphie sequentielle de l'Aptien du sous-
660 basin de Galvé (Province de Teruel, NE de l'Espagne). Bulletin de la Société
661 Géologique de France 172(4), 397–410.

662 Weisser, D., 1959. Acerca de la estratigrafía del Urgo-Aptense en las cadenas
663 Celtibéricas de España. Notas y comunicaciones del Instituto Geológico y
664 Minero de España 55, 17-32.

665

FIGURE CAPTIONS

Fig. 1 – A) Location of study area in eastern Spain and simplified geologic map of the central and eastern parts of the Galve sub-basin showing studied outcrops (modified from Canérot et al., 1979; Gautier, 1980 and Bover-Arnal et al., 2010). B) General stratigraphic framework for the Aptian in the Galve sub-basin. Identified ammonoid biozones are marked in grey (Weisser 1959; Moreno-Bedmar et al. 2009, 2010). Modified from Bover-Arnal et al. (2009, 2010). C) Schematic two-dimensional model displaying the Aptian lithofacies architecture, platform development and sequential evolution in the central Galve sub-basin. Based on Bover-Arnal et al. (2009). The situation of the cross-section A-A' is indicated in Fig. 1A.

Fig. 2 – A) Margin of the Camarillas-El Morrón platform (highstand normal regressive (HNR) of Depositional Sequence A displaying the landward onlapping of Las Mingachas platform (lowstand normal regressive (LNR) of Depositional Sequence B. B) Sequence stratigraphic interpretation of Figure 2A. Note the downlap and prograding clinoforms exhibited by the slopes of the Camarillas-El Morrón platform (HNR of Depositional Sequence A), and how the maximum regressive surface (MRS) superposes the subaerial unconformity (SU) towards the land resulting in a composite sequence boundary (SU+MRS). Observe also the flat-topped non-rimmed depositional profile exhibited by the Camarillas-El Morrón platform. See Fig. 1 for legend. Modified from Bover-Arnal et al. (2009, fig. 8 therein) relative to which the sequence boundary has been located at a slightly lower level, at the base of the uppermost thickest limestone unit, such that the whole of the uppermost limestone body is regarded as a transgressive unit.

Fig. 3 – A) Las Mingachas prograding platform (LNR of Depositional Sequence B), B) Sequence stratigraphic interpretation of Figure 3A. Note the flat-topped non-rimmed depositional profile of Las Mingachas platform and how the facies change laterally from those of shelf settings to slope environments. The massive lithofacies (above) are parautochthonous, while the lithofacies with a nodular aspect (below) correspond to resedimented deposits. See Figure 1 for legend. Modified from Bover-Arnal et al. (2009). C) Complete photo-panorama of Las Mingachas platform, taken from the NE, showing the complete platform-slope-basin transition.

Fig. 4 – A) View of the composite stratigraphical surface (SU+MRS) that caps the Camarillas-El Morrón platform near Camarillas village (Fig. 1A). Bedding is almost vertical. B) Sequence stratigraphic interpretation of Figure 4A. Note that the transgressive system (T) of Depositional Sequence B onlaps the composite sequence boundary. See Fig. 1 for legend. Modified from Bover-Arnal and Salas (2010).

Fig. 5 - A) Panoramic view of the Camarillas-El Morrón platform-to-basin transition area situated in the central part of the Galve sub-basin (west of Miravete de la Sierra; Fig. 1A). B) Sequence stratigraphic interpretation of Fig. 5A. Modified from Bover-Arnal et al. (2009; fig. 6 therein), as explained in the caption to Fig. 2.

Fig. 6 - A) *Toucasia carinata* (note attachment by the larger, left valve in the extracted specimen at left and the simple posterior myophoral ledges in both valves of the articulated specimen shown in section next to the latter in the rock face). B) *Polyconites hadriani*, natural section across an articulated specimen (note reflexed posterior myophore at left in the upper, left valve; see also Skelton et al., 2010).

Fig. 7 – A) and B) Plots of the first two axes of the principal component analysis (PCA) performed on 10 samples using 7 biological variables: (A) correlation circle; (B) sample scatter. C) and D) Cluster analyses using the Ward method (Saporta, 1978), based on the first three axes of the PCA: (C) clustering of

variables in two groups; (D) clustering of samples into two groups – representing relatively dense-, and loose shell assemblages, respectively. Note that the fabric clusters in (D) do not correspond exactly to the taxonomically identified biofacies recognized in the field: whereas both samples of the *Polyconites* biofacies comprise dense clusters, six of the samples from the *Toucasia* biofacies form loose assemblages, while two constitute dense assemblages, as discussed in the text.
Key to abbreviations: Avsize = average size of rudist shells; Maxsize = Maximum size of rudist shells; Minsize = Minimum size of rudist shells; Density = packing density; Packind = packing index; Skeletal = contribution of macro-elements of rudist versus matrix; Coverage = coverage of rudist shells.

Fig. 8 – A) View northwards along the ridge beside Camarillas village showing, in the foreground, the steeply dipping beds (younging to the right) comprising the internal zone of the Camarillas-El Morrón platform. The two units (unit 1 and unit 2) visible here within the succession are separated by a composite stratigraphical surface, formed by a subaerial unconformity superposed by a maximum regressive surface (SU+MRS). The top of unit 2 – top of the platform – is capped by another, similar composite stratigraphical surface (SU+MRS). B) Leached rudist inner shell and geopetal cavity cements replaced by red-stained fine- grained internal sediment, in unit 1. C) Sedimentary log of the section here, with units 1 and 2 indicated; modified from Bover-Arnal et al. (2009). The downcutting boundary between Sequences B and A shown in Fig. 4 is visible beyond.

Fig. 9 – Internal platform (unit 1) biofacies near Camarillas village. A) *Toucasia* dominated platform-top association, seen in vertical section (bedding is almost vertical), hammer shaft is 36 cm long. B) Detail of Fig. 9A, centimetre scale at right. C) Photomicrograph of fine bioclastic wackestone microfacies, containing scattered sponge spicules, benthic foraminifers (including fragments of orbitolinids), ostracode valves and other, indeterminate angular bioclasts ; D) Photomicrograph of medium grained packstone microfacies, containing angular and superficially bored, and/or microbially coated bioclasts, including those derived from echinoids, rudists, benthic foraminifers and other, indeterminate

forms. The thin section photomicrographs are in plane-polarised light and 3.4 mm across. bf = small benthic foraminifer, e = echinoid, or = orbitolinid, os = ostracode, r = rudist, sp = sponge spicule.

Fig.10 – Internal platform (unit 2) biofacies near Camarillas village. A) *In situ* cluster of *Toucasia carinata*, viewed from above (2 Euro coin for scale, 25 mm diameter). B) *Toucasia* encrusting the hardground surface that caps one of the minor cycles. C) Small monopleurid, *Mathesia*, right valve; with 2 Euro coin for scale, 25 mm diameter. D) Natural vertical section across autochthonous branching corals, with centimetre scale at right.

Fig.11 – Platform margin limestones; A, B, E and F at Las Mingachas locality, C and D at El Morrón. A, B, C and E in natural vertical section. A) Branching (phaceloid) corals covered by bioclastic floatstone. B) Densely clustered *Polyconites hadriani* in life position. C) Floatstone showing *Polyconites hadriani* valves in section. Note, in the centre, the antero-posterior section across both valves of an articulated specimen, viewed towards dorsal side; arrows indicate the two myophores in the left valve (above). Scale, 1 Euro coin, diameter 23 mm. D) Autochthonous cluster of *Toucasia* encrusting the hard top of the platform margin, viewed from above. E) Clustered *Chondrodonta* (elongated oyster-like shells) mixed with *Polyconites*. F) Section across left valve of *Caprina parvula;* note pallial canals with bifurcating laminae (arrowed). Scale to right in A, E and F in cm.

Fig. 12 – Natural vertical section across autochthonous polyconitid dominated platform-margin association: individuals are mutually attached (from Las Mingachas locality).

Fig. 13 – Photomicrographs of microfacies of platform margin. A) Camarillas-El Morrón platform – transverse section of microbially coated, phaceloid corallite in a poorly-sorted wackestone matrix. B) Las Mingachas platform – poorly-sorted wackestone with plates and spines of echinoids, rudist fragments, small benthic foraminifers and other, indeterminate bioclasts. Both photomicrographs are in

plane-polarised light and 3.4 mm across. c = coral, e = echinoid, ef = encrusting foraminifer, r = rudist.

Fig. 14 – A) and B) Photomicrograph in plane-polarised light of slope microfacies: (A) Camarillas-El Morrón platform – floatstone matrix of fine-grained, poorly-washed grainstone to packstone with bioclasts of echinoids, gastropods, small benthic foraminifers and other, indeterminate bioclasts; (B) Las Mingachas platform – rudist and coral floatstone with matrix of fine-grained, wackestone to packstone with other bioclasts including those of echinoids, thin-shelled bivalves and small benthic foraminifers. C) Phaceloid corals associated with *Polyconites hadriani*, together with displaced *Toucasia*, in a clinoformal lithosome at El Morrón locality. Frame in A and B is 3.4 mm across. b = small bivalve, bf = small benthic foraminifer, c = coral, e = echinoid, g = gastropod.

Fig. 15 – Platform to uppermost slope transition facies at Las Mingachas. A) Cluster of displaced individuals of *Polyconites hadriani*. B) *Polyconites hadriani* preserved in life position (viewed from above), densely clustered with their feeding margins oriented sub-vertically, like recent flat oysters. C) Natural vertical section across autochthonous platy coral. D) *In situ* overturned bouquet of *Polyconites*. Scale in cm.

Fig. 16 – Cluster of live *Crassostrea* sp., in life position on mud flat, viewed from above, Florida, USA. Scale bar = 7 cm.

TABLE CAPTIONS

Table 2. Quantitative fabric data (see Table 1 for definitions of variables). Samples Cam 1-6 are from the HNR (Sequence A) at Camarillas, with Cam 1, 2 from unit 1 and Cam 3-6 from unit 2 (Cam 3, 4 from *Toucasia* clusters and Cam 5, 6 from *Mathesia* clusters within the *Toucasia* biofacies); and Mir 1, 2 coming from the *Toucasia* biofacies, and Mir 3, 4 from the *Polyconites* biofacies, respectively, in the LNR (Sequence B) at Miravete.

Table 1.

Measures obtained for quantitative analysis of rudist assemblages

All data were obtained from field macro-photographs of exposed natural rock surfaces oriented either parallel or perpendicular to bedding and analyzed by image analysis using ImageJ: Image Processing and Analysis in Java "http:/rsbweb.nih.gov/j/"

Shell size is the averaged linear measurement of shells exposed in transverse section and is recorded together with maximum and minimum measurements.

Packing density is the number of individuals found on a reference surface, in this study normalized to 0.1 m^2, as used for the study of living benthic organisms on soft substrates (Pérés, 1961).

Packing index is the quotient of the number of mutual contacts between shells (usually involving cementation) to the total number of shells along a transect line, expressed as a percentage; it is based on the index given by Flügel (1982, pp. 90, 215) to represent grain packing in sedimentary rocks.

Coverage is measured either as the percentage intercept with shells along a transect parallel to bedding or as the amount of shell cover versus matrix calculated by image analysis on a given surface.

Skeletal contribution is the percent of macro-shelly material versus sedimentary matrix estimated by image analysis of field photographs.

Table 2.

Samples	Packing Density (per 0.1 m^2)	Minimum size (cm)	Maximum size (cm)	Average size (cm)	Skeletal contribution (%)	Coverage (%)	Packing Index (%)
Cam 1	5.8	1	3.7	2.1	13.7	29.4	30.2
Cam 2	3.4	0.7	3.3	2.1	9	28	18.8
Cam 3	8	0.7	3.4	1.6	12.7	27.9	26
Cam 4	5.1	1.8	5.4	2.9	18.8	46	37
Cam 5	7.4	0.9	4.6	1.7	12.1	24.4	47
Cam 6	15.9	0.8	1.7	1.1	16.8	32.4	49.6
Mir 1	6.3	0.8	3.2	1.8	8	23	17.6
Mir 2	3.2	1.4	3.5	2.3	10.2	23.8	25.6
Mir 3	26.3	0.8	3.9	2.1	28.7	58.5	61.6
Mir 4	17.5	0.9	2.6	1.5	20.7	42.1	43

Figure 1

Click here to download high resolution image

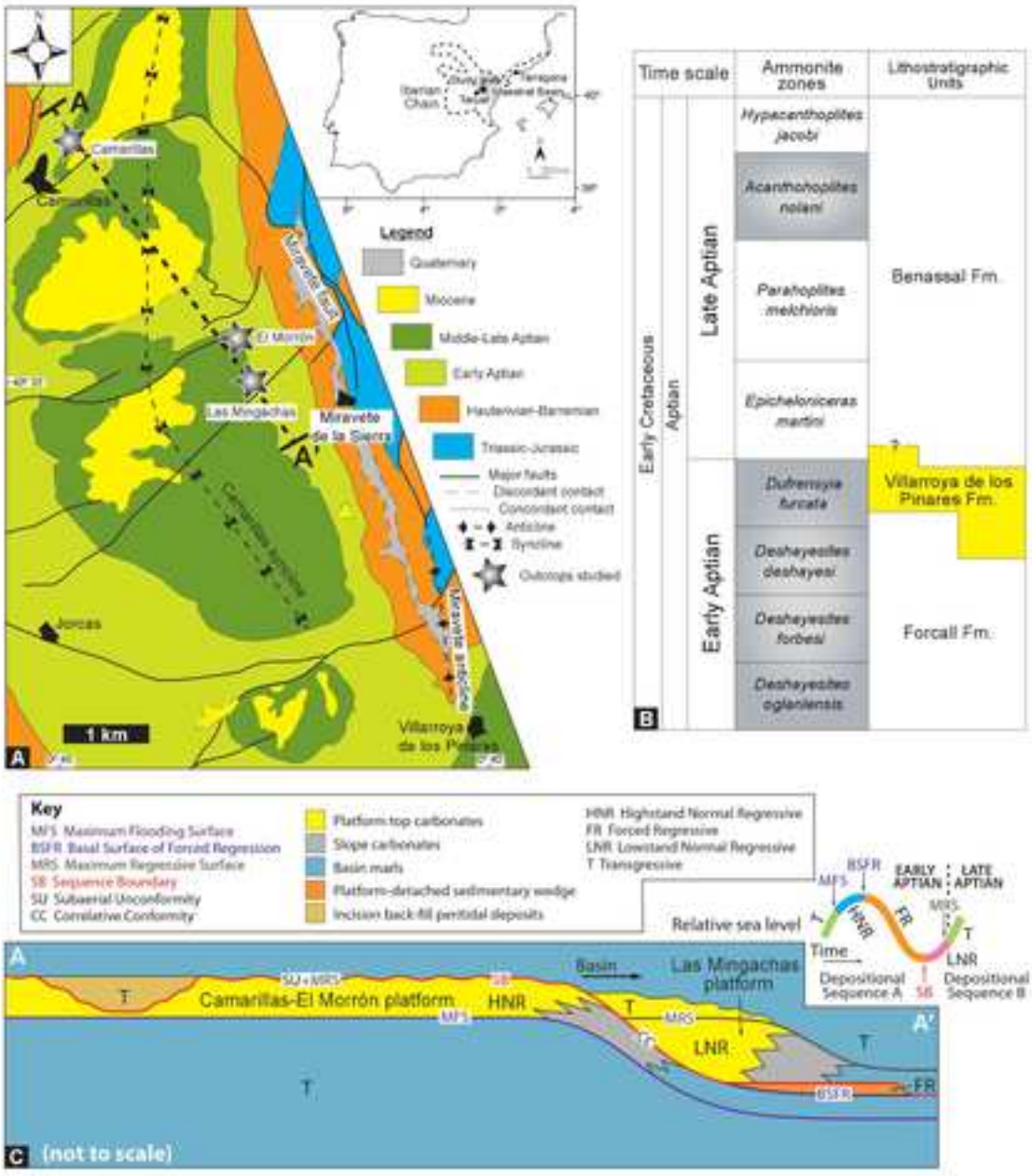

Figure 2

Click here to download high resolution image

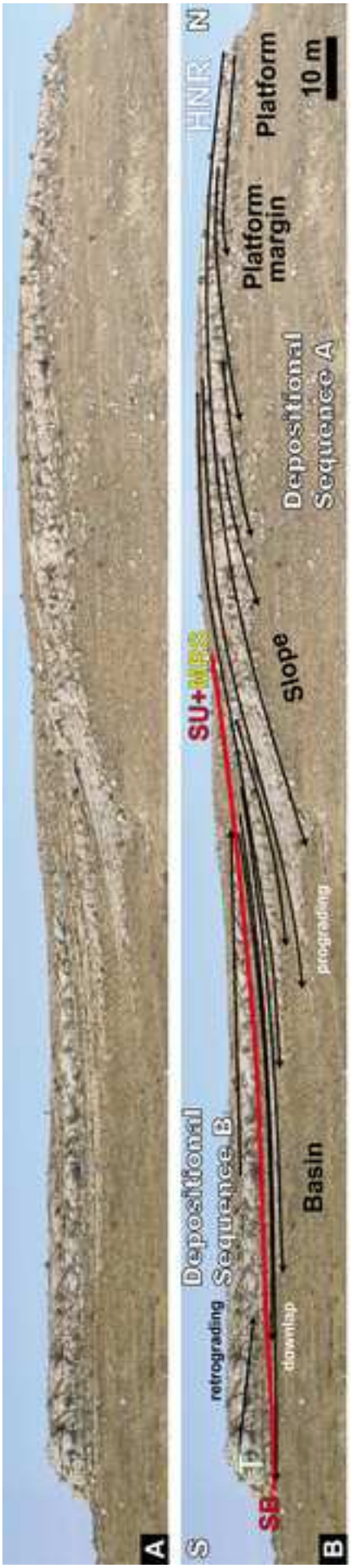

Figure 3

Click here to download high resolution image

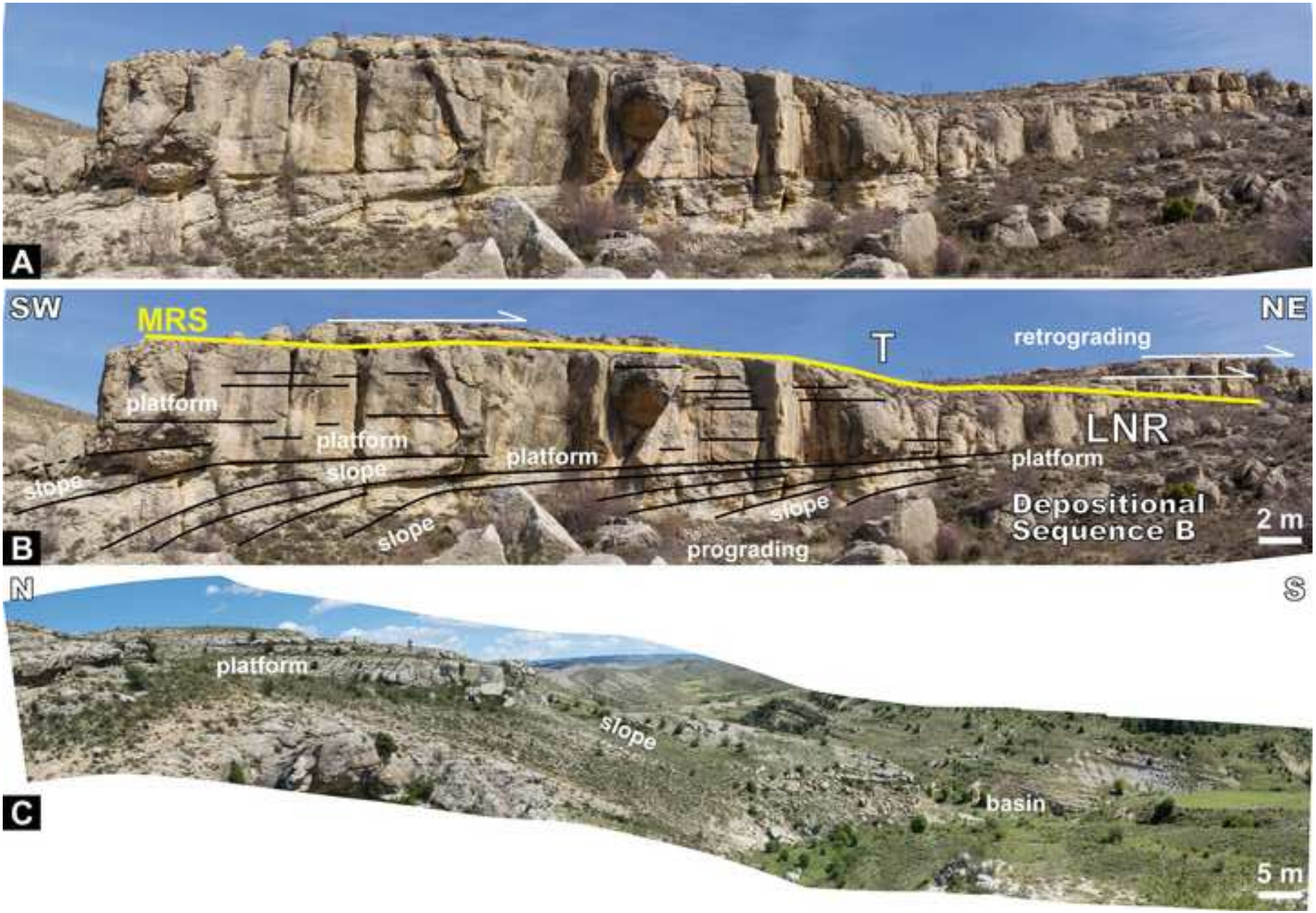

Figure 4

Click here to download high resolution image

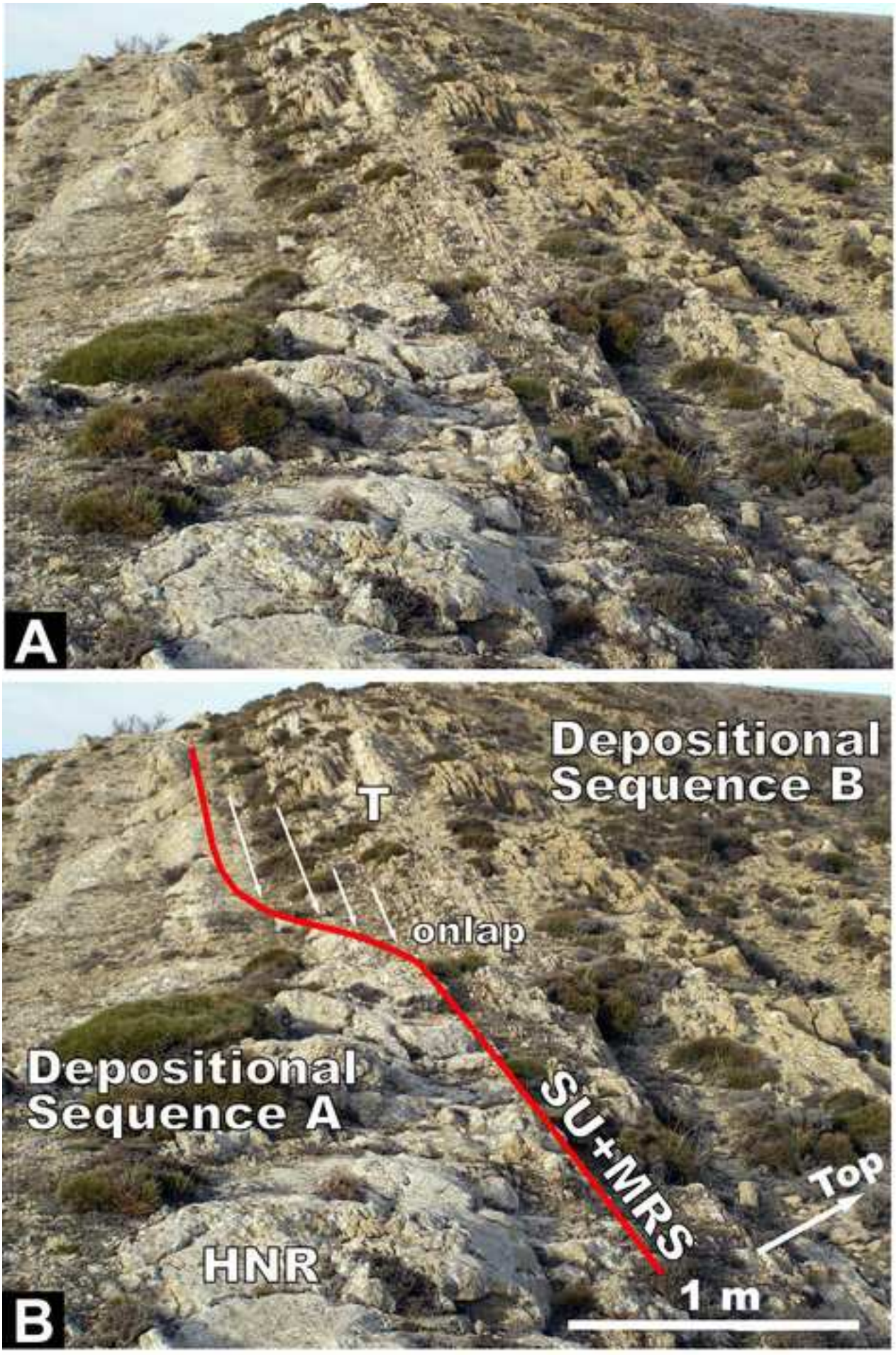

Figure 5

Click here to download high resolution image

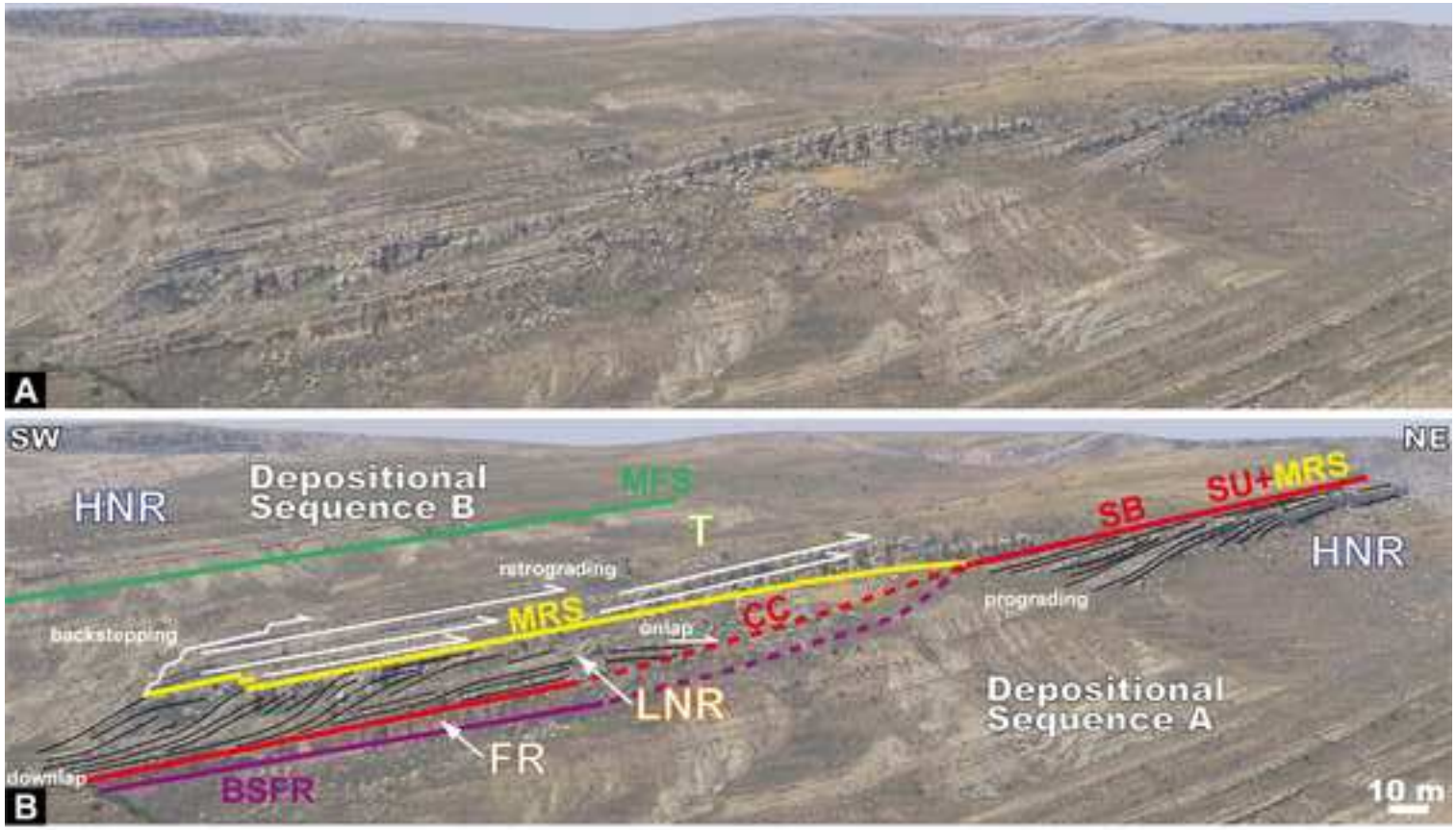

Key

HNR: Highstand Normal Regressive

FR: Forced Regressive

LNR: Lowstand Normal Regressive

T: Transgressive

BSFR: Basal Surface of Forced Regression

SB: Sequence Boundary

MRS: Maximum Regressive Surface

MFS: Maximum Flooding Surface

CC: Correlative Conformity

SU: Subaerial Unconformity

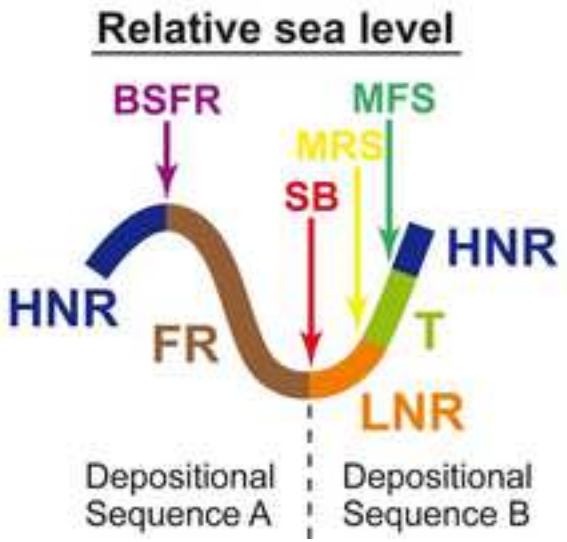

Figure 6

Click here to download high resolution image

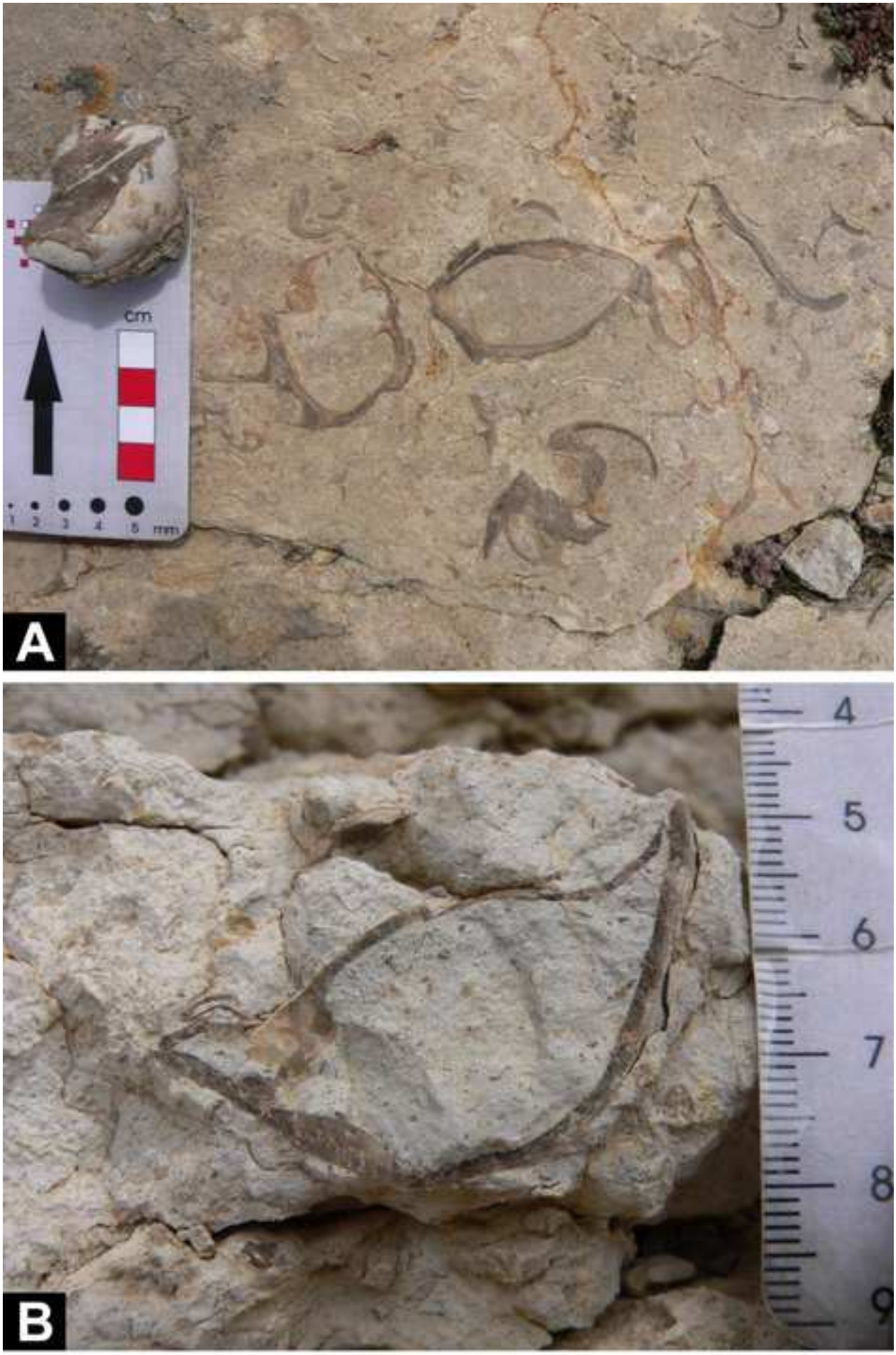

Figure 7

Click here to download high resolution image

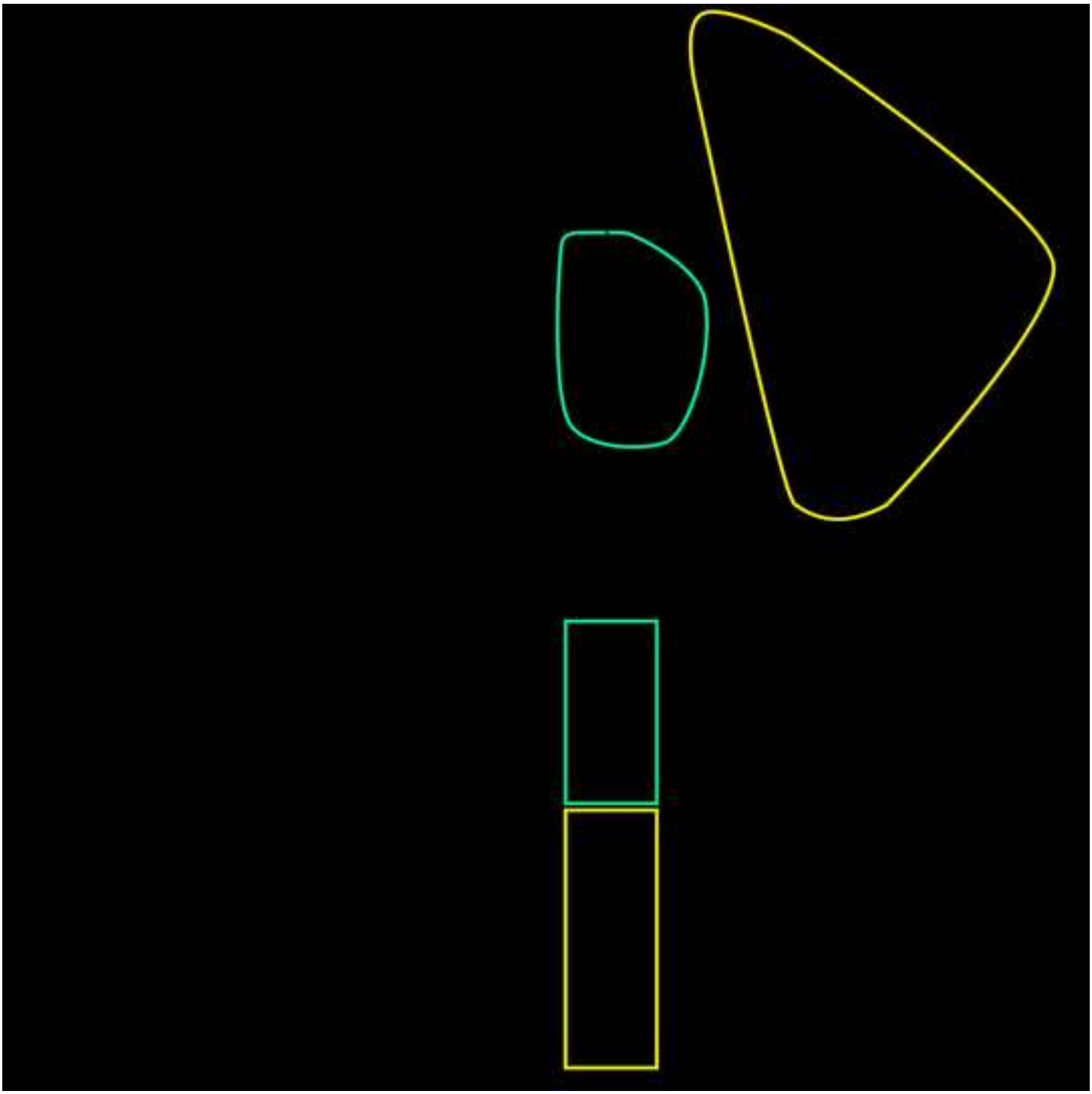

Figure 8

Click here to download high resolution image

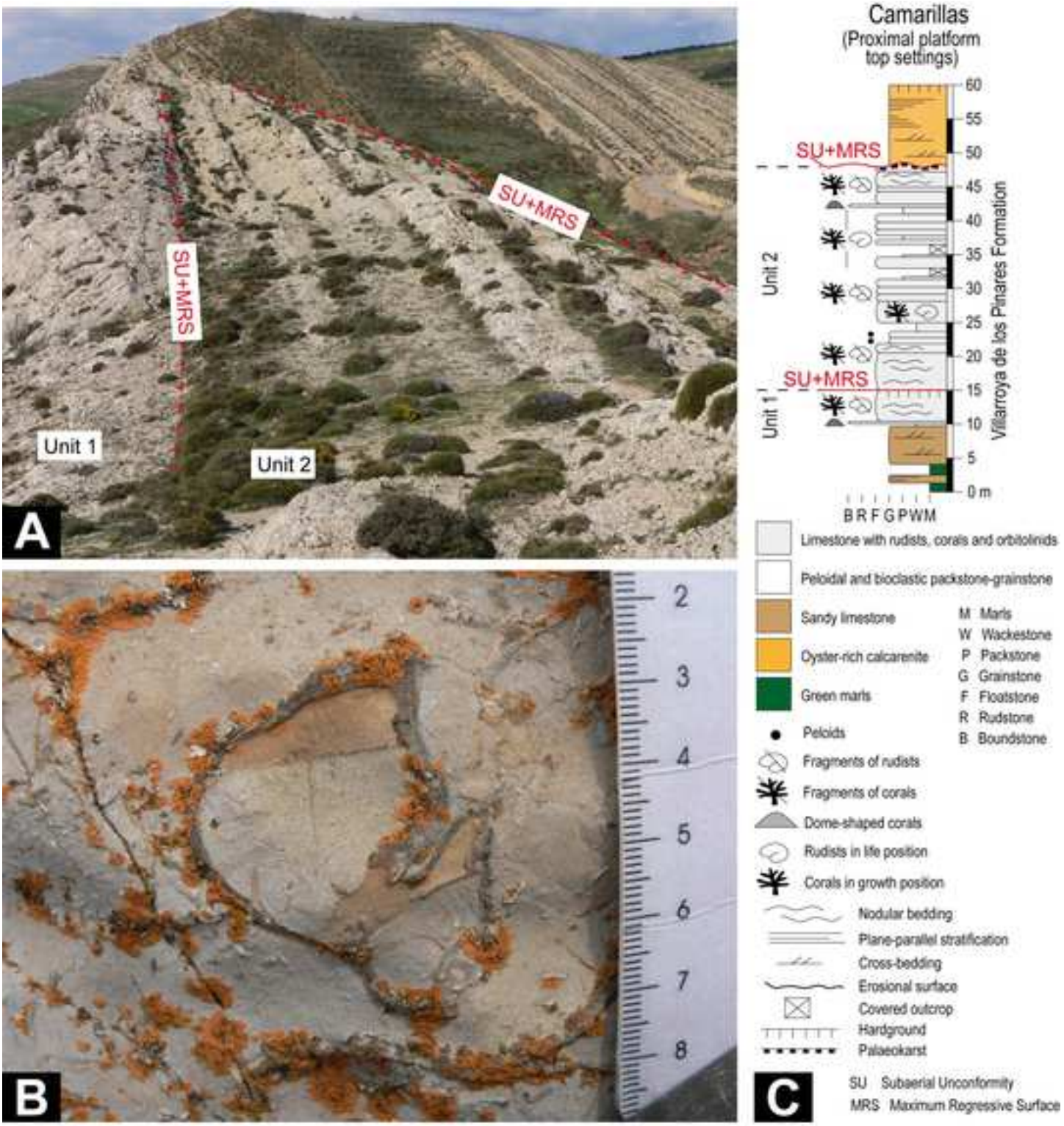

Figure 9

Click here to download high resolution image

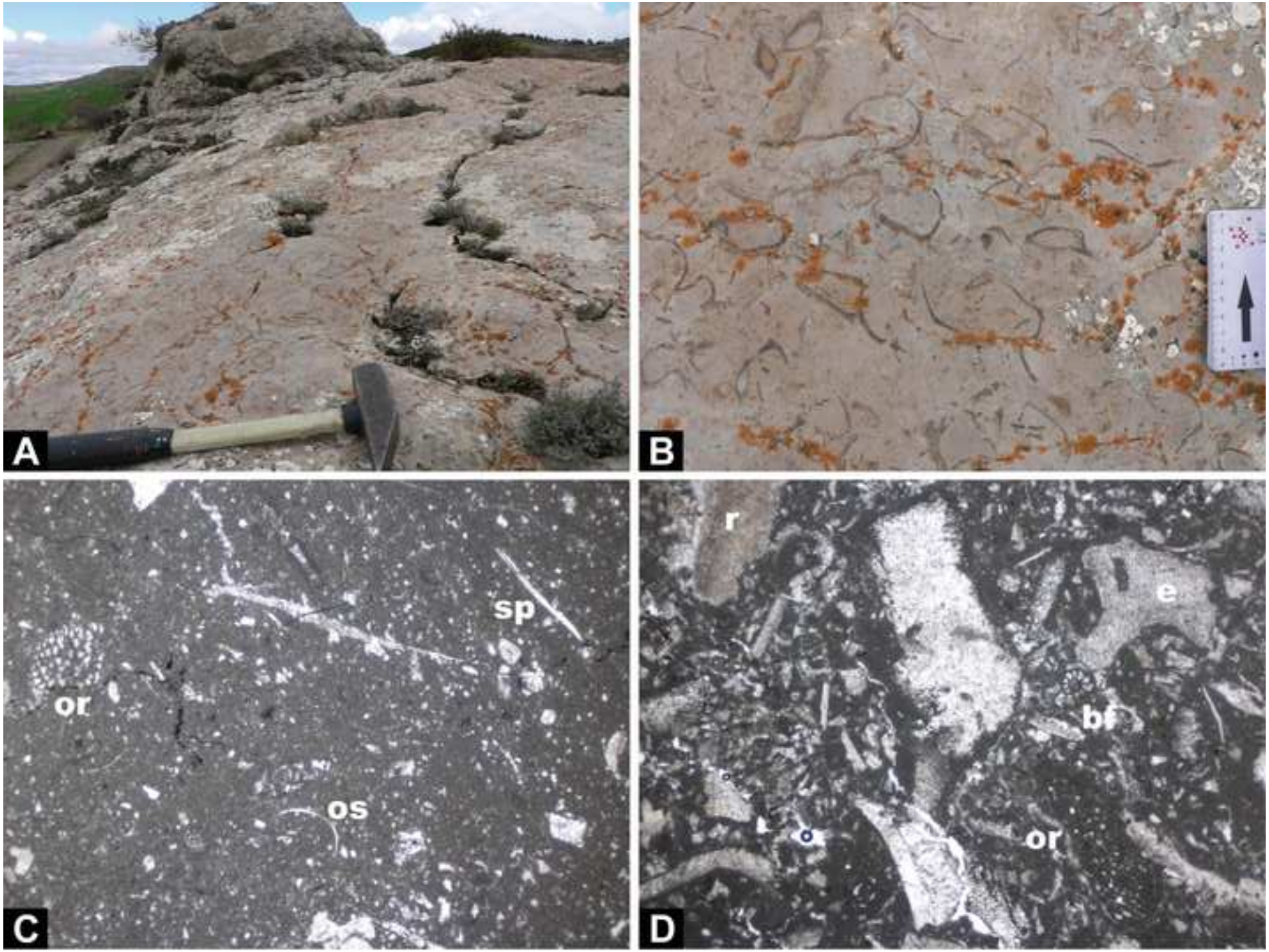

Figure 10

Click here to download high resolution image

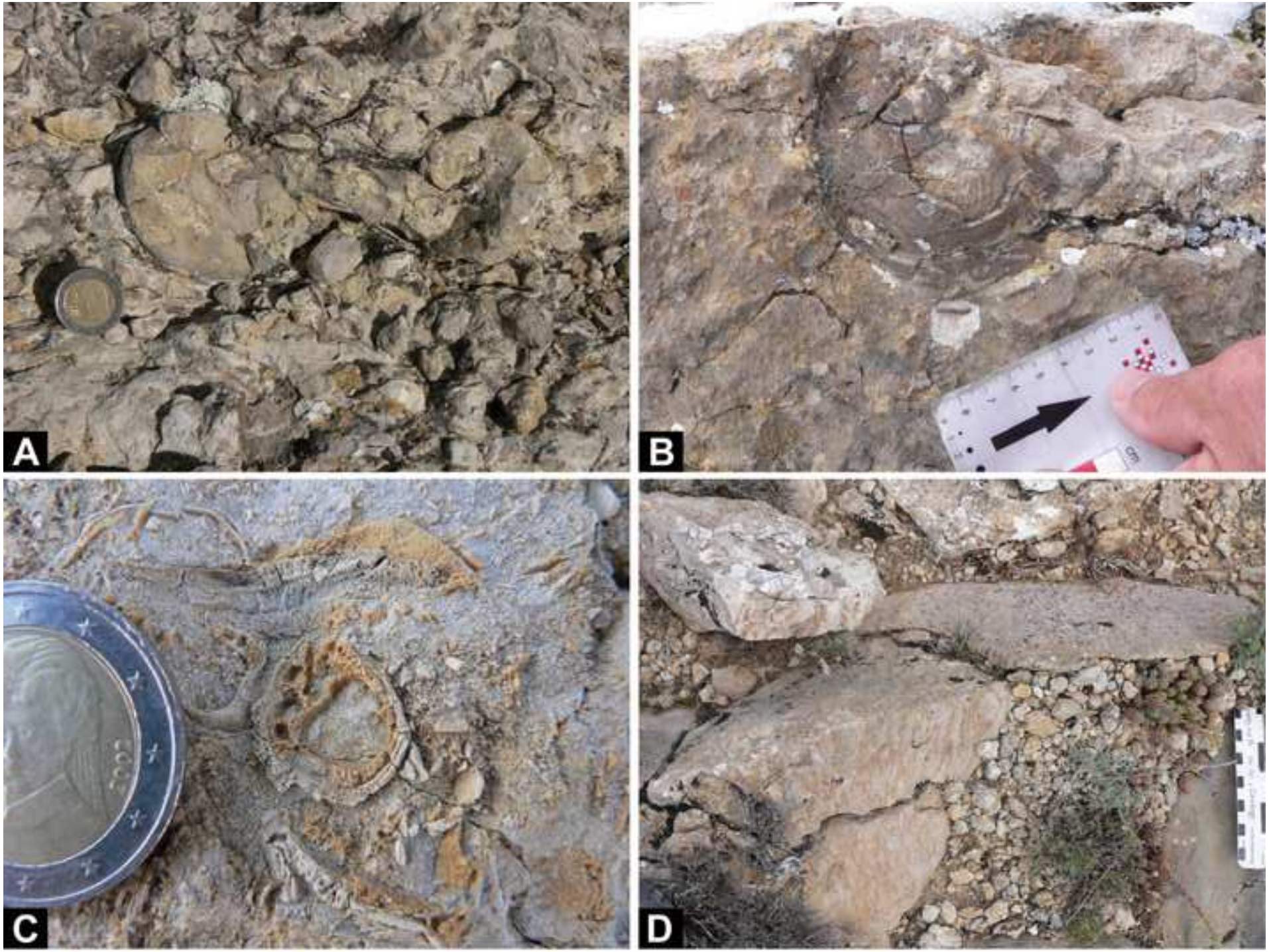

Figure 11
Click here to download high resolution image

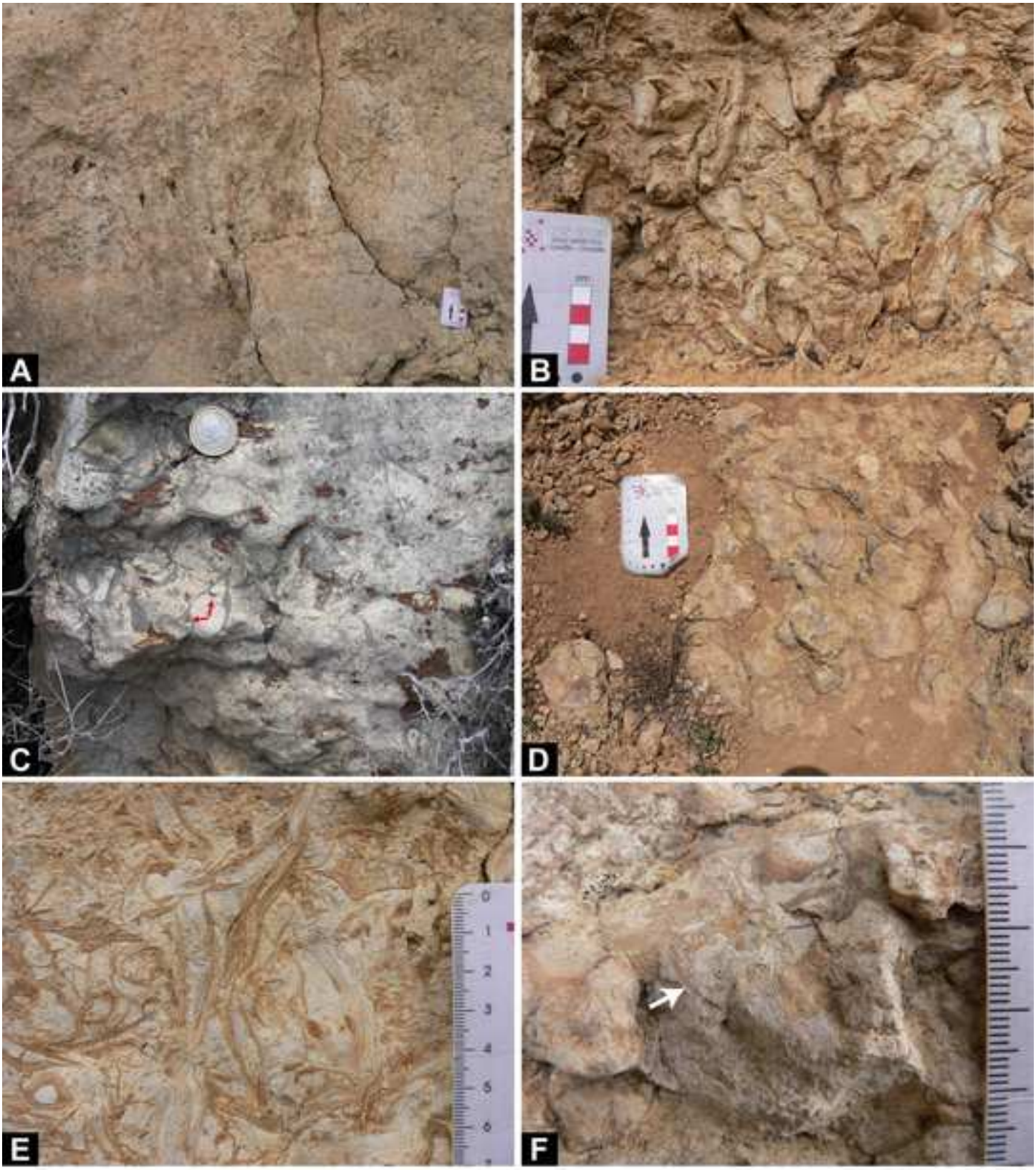

Figure 12

Click here to download high resolution image

Figure 13

Click here to download high resolution image

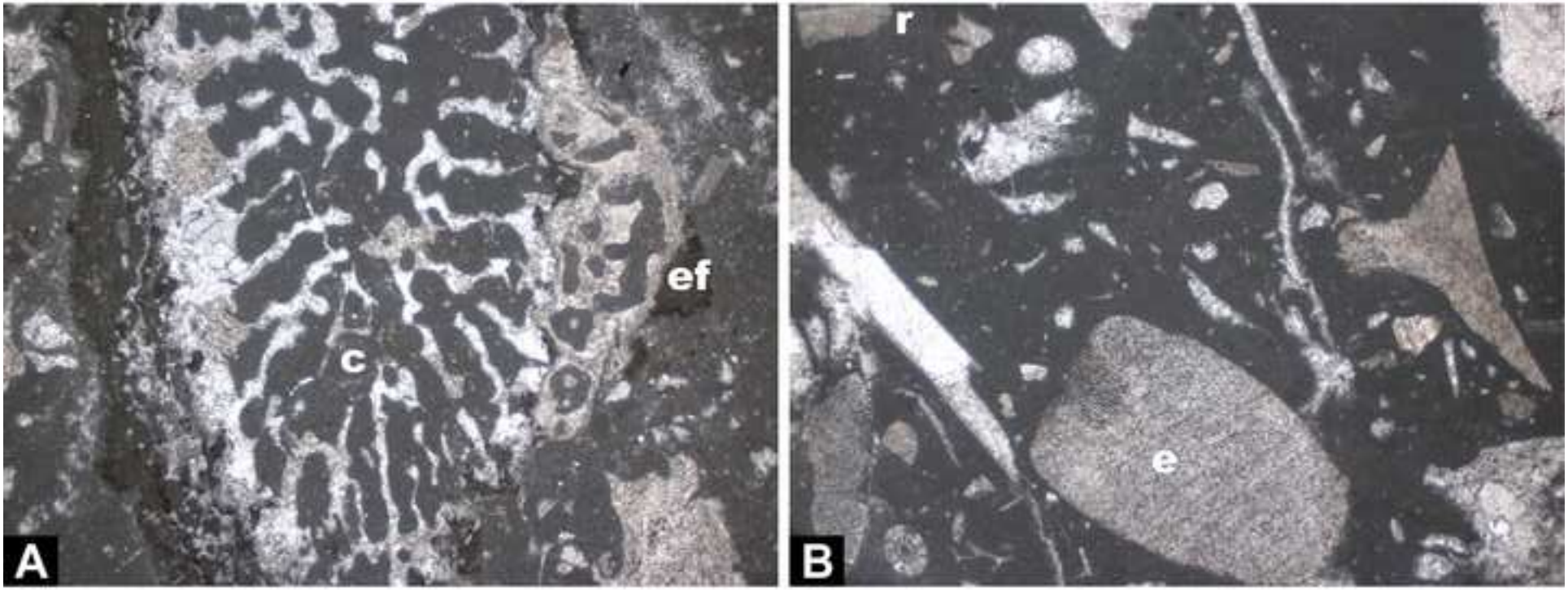

Figure 14

Click here to download high resolution image

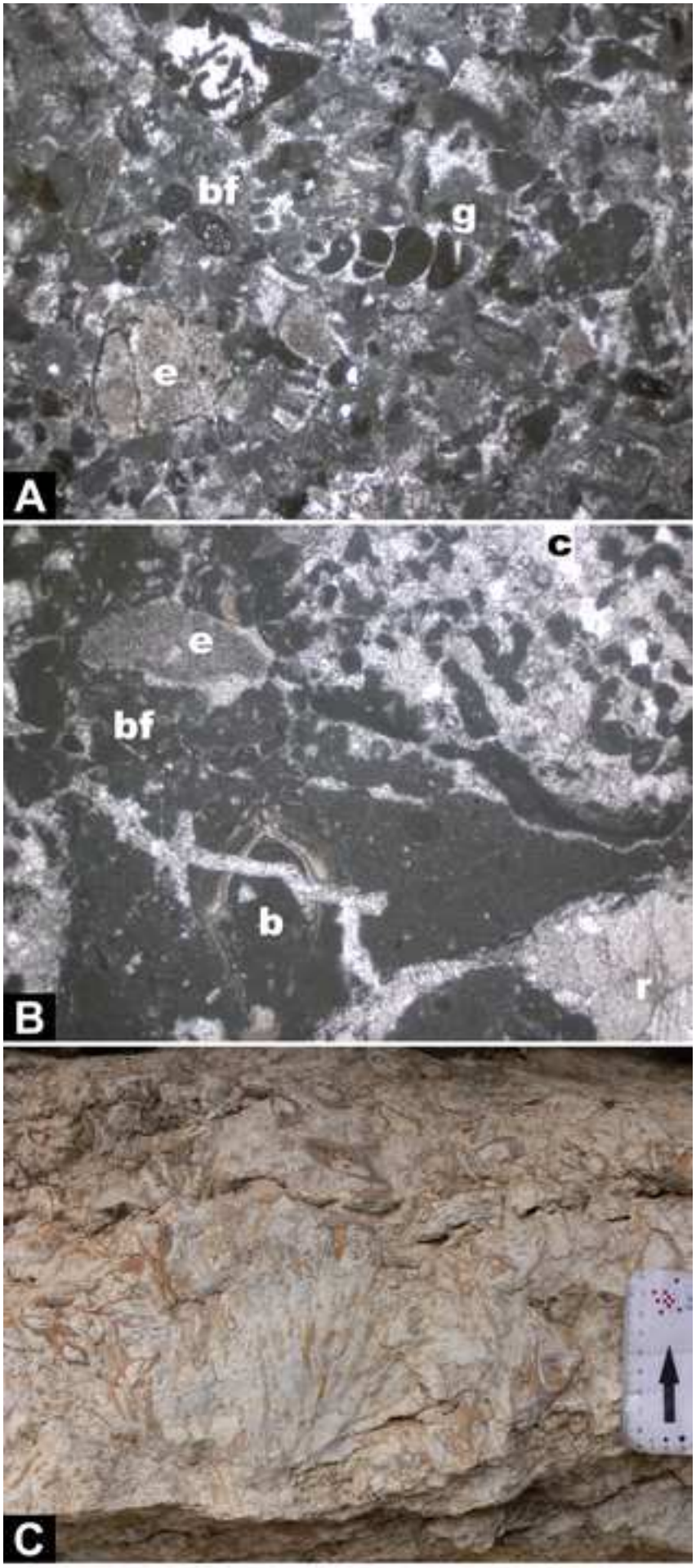

Figure 15

Click here to download high resolution image

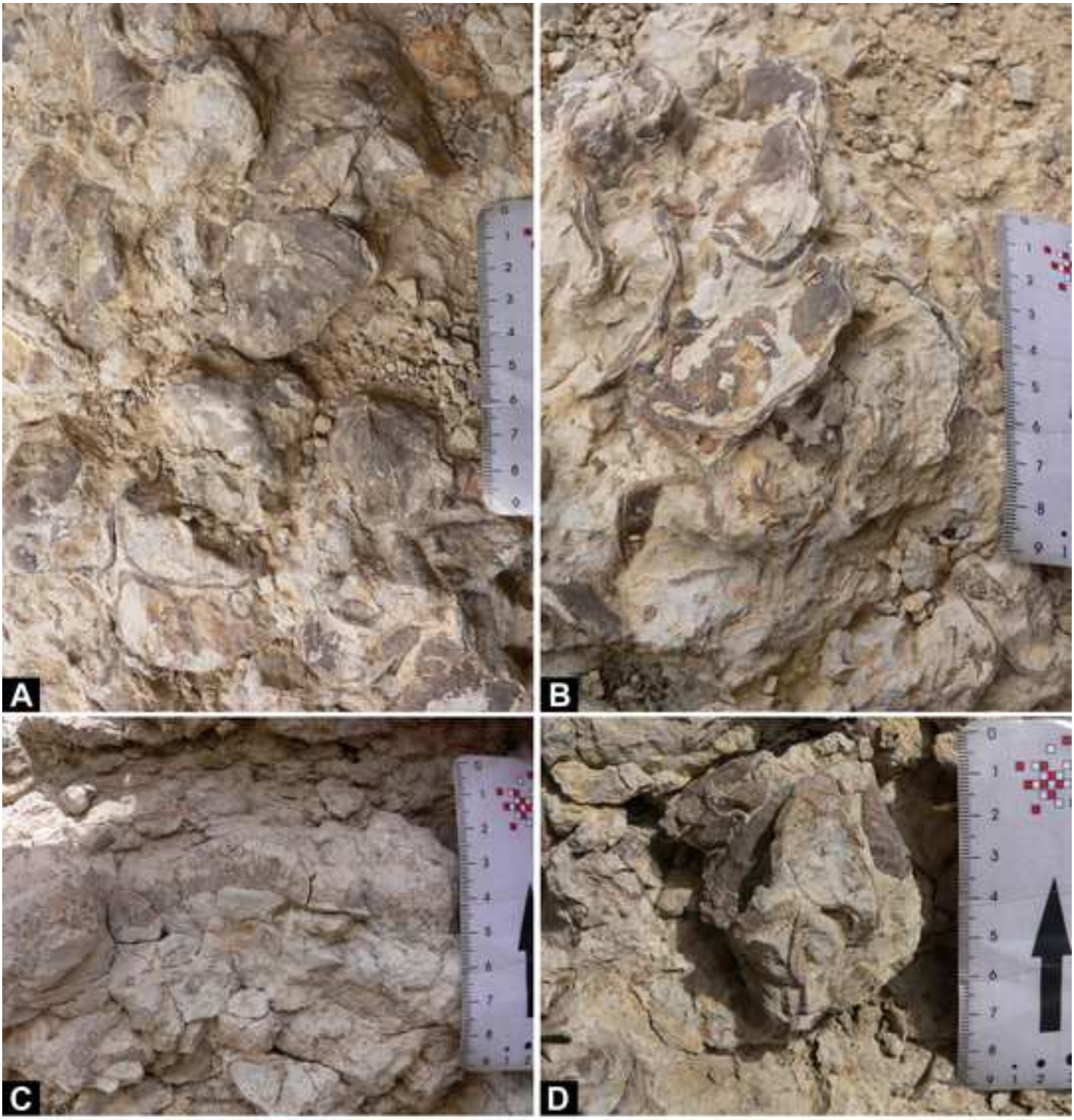

Figure 16
Click here to download high resolution image

Dear editor,

Please find enclosed our submission of the manuscript, '**Depositional biofacies model for Aptian carbonate platforms of the western Maestrat Basin (Iberian Chain, Spain): a case history of post OAE1a Iberian platforms**' by Gili et al., which we would like to publish as a research paper in Palaeogeography Palaeoclimatology Palaeoecology.

We think this study meets the scope of this journal and furthermore represents a multidisciplinary approach combining fields of palaeontology, stratigraphy, and sedimentology. General understanding of how environmental factors could determine the distribution of rudist bivalves on carbonate platforms are very limited. In this publication after summarising the geological context within which two platform sequences of late Early Aptian age developed, we describe the biofacies in both quantitative and qualitative terms and then discuss the ambient environmental conditions in which they formed and the palaeoecology of the rudist bivalves that constitute their main macrobiotic elements.